polysaccharides

MDPI

Review

Crystallinity Changes in Modified Cellulose Substrates Evidenced by Spectral and X-Ray Diffraction Data

Magdalena-Cristina Stanciu [1,*], Fulga Tanasă [2] and Carmen-Alice Teacă [3,*]

[1] "Petru Poni" Institute of Macromolecular Chemistry, Natural Polymers, Bioactive and Biocompatible Materials Department, 41A, Gr. Ghica-Voda Alley, 700487 Iasi, Romania
[2] "Petru Poni" Institute of Macromolecular Chemistry, Polyaddition and Photochemistry Department, 41A Gr. Ghica-Voda Alley, 700487 Iasi, Romania; ftanasa@icmpp.ro
[3] "Petru Poni" Institute of Macromolecular Chemistry, Advanced Research Center for Bionanoconjugates and Biopolymers, 41A Gr. Ghica-Voda Alley, 700487 Iasi, Romania
* Correspondence: cstanciu@icmpp.ro (M.-C.S.); cateaca14@yahoo.com (C.-A.T.)

Abstract: The crystallinity of cellulose substrates is a key factor in their processability, as well as an indication of their susceptibility to undergo sensitive reactions (such as enzymatic saccharification) with high yields. FT-IR and X-ray diffraction spectroscopy are useful, reliable, and easy-to-reach solid-state characterization methods for assessing the crystallinity of different cellulose substrates including wood and wood-based materials. Due to their specific methodology, they can be used to analyze not only starting materials and their final products but also intermediates. Data obtained by these methods substantiated the structural changes in cellulose substrates, as well as the alterations that occurred in their supramolecular architectures. The conversion of crystalline cellulose I into amorphous cellulose II during enzymatic saccharification, with or without pre-treatment (solubilization in ILs), was evidenced beyond any reasonable doubt by FT-IR and XRD experimental results. Enzyme hydrolysis rates of the ILs-treated cellulose substrates can be significantly increased, as evidenced by reducing sugar yields. Crystallinity index values for cellulose of different origins (initial, pre-treated with ILs, and hydrolyzed with enzyme, as well as cellulose submitted to one-pot procedure with ILs and enzyme) can be determined using FTIR and X-ray diffraction data and discussed for comparison purposes. The same solid-state characterization methods can be also successfully employed for investigation of surface changes, expressed as cellulose crystallinity, in wood samples before and after impregnation with natural-based products, as well as under biodegradation conditions in soil burial tests.

Keywords: cellulose substrate; cellulase; ionic liquid; natural-based products; structural changes; FTIR spectroscopy; X-ray diffraction; crystallinity index

check for updates

Academic Editors: Adrian C. Puiţel and Mircea Teodor Nechita

Received: 30 December 2024
Revised: 6 March 2025
Accepted: 2 April 2025
Published: 4 April 2025

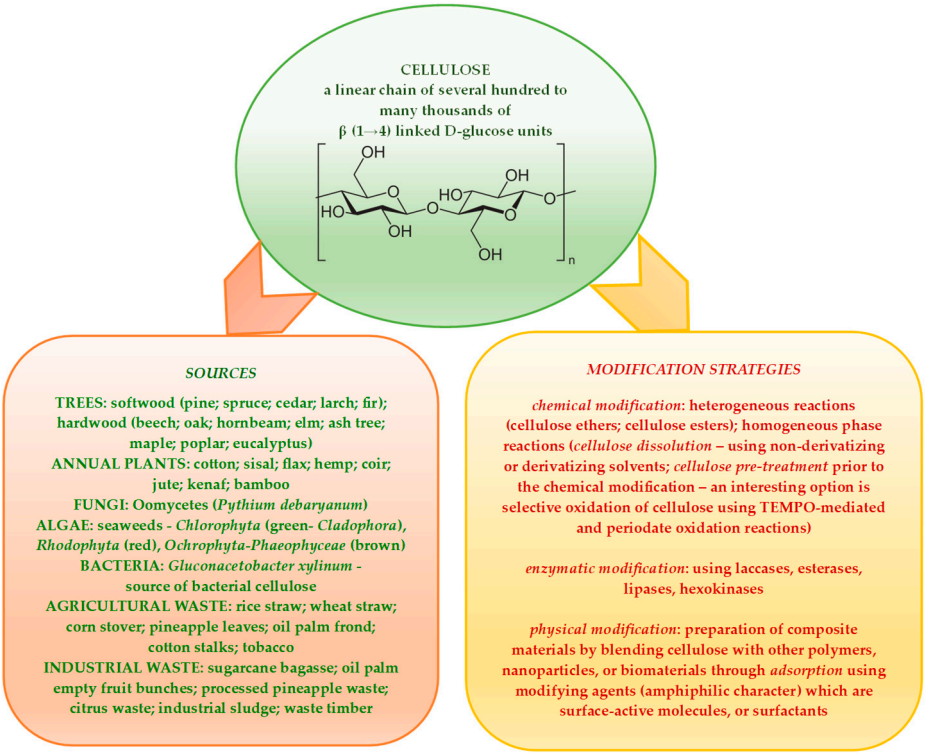
Citation: Stanciu, M.-C.; Tanasă, F.; Teacă, C.-A. Crystallinity Changes in Modified Cellulose Substrates Evidenced by Spectral and X-Ray Diffraction Data. *Polysaccharides* **2025**, *6*, 30. https://doi.org/10.3390/polysaccharides6020030

Copyright: © 2025 by the authors. Licensee MDPI, Basel, Switzerland. This article is an open access article distributed under the terms and conditions of the Creative Commons Attribution (CC BY) license (https://creativecommons.org/licenses/by/4.0/).

1. Introduction

Lignocellulosic biomass, which is considered and acknowledged to be one of the most valuable natural resources of the future, is renewable, carbon neutral, and widely available in different forms. Cellulose—the main polymer component of vegetal substrates such as wood, straw, crop residues etc.—contributes, along with lignin and hemicelluloses, to the complex structure of lignocellulosic materials fit for processing into a large scale of value-added products that are essential to societal development [1–5]. A comprehensive representation of the cellulose structure and its main sources (with cellulose polymer components having varying degrees of polymerization and crystallinity), alongside the

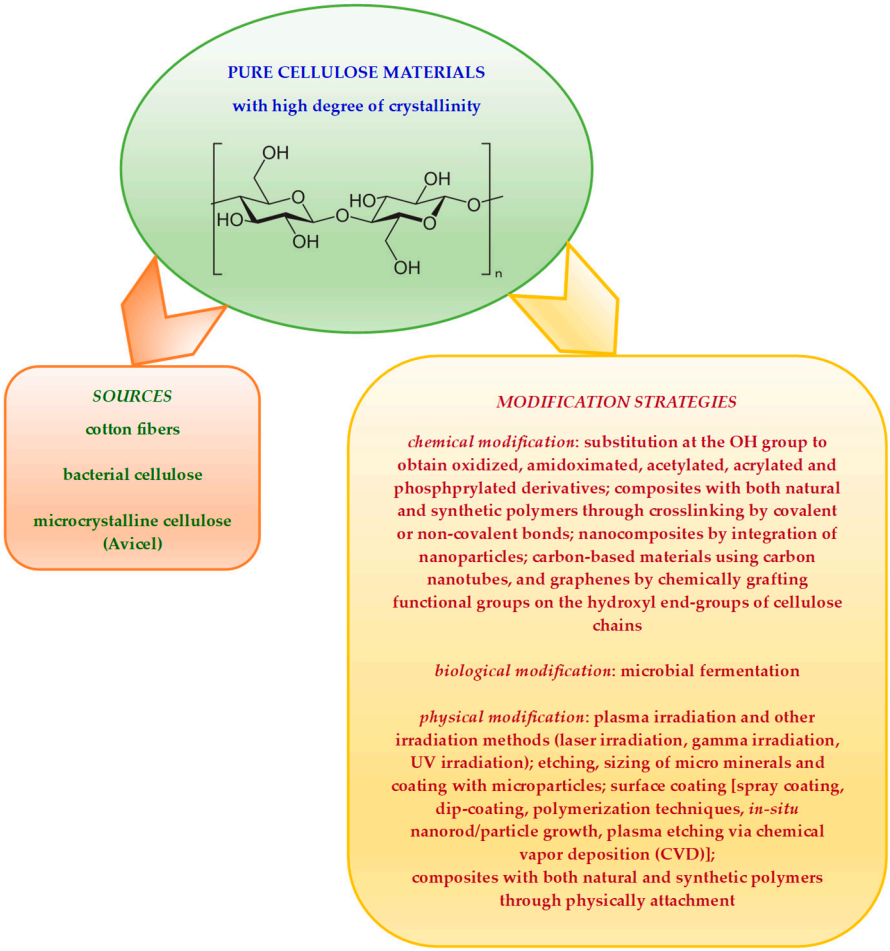
modification strategies applied for highly engineered cellulose derivatives, is presented in Scheme 1 [6–11].



Scheme 1. A detailed schematic of cellulose chemical structure, its main sources, and modification strategies employed to obtain advanced cellulose derivatives.

Cellulose, one of the most amazing polysaccharides in nature, is structurally organized in lignocellulosic biomass sources, mainly wood fibers, as microfibrils that combine large ordered crystalline areas with low-ordered non-crystalline (amorphous) domains [12]. The latter are observed mainly at the outer side of these microfibrils as a consequence of the structural embedding of crystalline cellulose within the network formed with the other wood polymer constituents, namely hemicelluloses and lignin, which are mostly amorphous in nature. Such domains can display both paracrystalline and fully amorphous cellulose forms, noting that thin paracrystalline layers are present on the surface of the cellulose crystals [13].

Pure cellulose materials present multiple hydrogen bonds and a high degree of crystallinity as well as hydrophobicity [14–16]. All these contribute to their low saccharification efficiency. A graphical representation of some methods successfully employed for pure cellulose-derived materials modification is given in Scheme 2.



Scheme 2. Some examples of modification strategies employed to obtain advanced cellulose derivatives from pure cellulose-derived materials.

2. Crystallinity in Cellulose Substrates—Towards Its Changes Through Applying Pre-Treatment Strategies

The chemical composition of different lignocellulosic biomass sources and the crystallinity of the corresponding cellulose represent very important features when different properties (e.g., physical, chemical, mechanical) of cellulose-based materials need to be evaluated in processing biomass sources (e.g., forestry-wood, agricultural feedstocks, agro-industrial residues) [17]. The biomass may be intended for various applications, mainly production of biofuels [3,18], chemicals, and materials [1,3,4,19,20]. In this context, it is well known that lignocellulosic fibers with high crystallinity have good dimensional stability, high density, and tensile strength, but reduced swelling ability and low chemical reactivity. This is the main issue that has to be addressed to improve their processability.

Biorefinery, an emerging wholistic concept in biomass processing, involves the efficient conversion of renewable biomass into biofuels and chemicals. It evolves in stages: firstly, the effective fractionation of biomass into its main constitutive polymers, namely cellulose, hemicelluloses, and lignin; and secondly, the sustainable hydrolysis of cellulose to monosaccharides, mainly glucose. This process represents the most important entry point into a biorefinery scheme based on polysaccharides [2,21–24]. Figure 1 gives a schematic overlook of the main strategies used for biomass pre-treatment [25–30] in order to overcome its low chemical reactivity and facilitate access to its main structural polymer components, mainly cellulose. As a consequence, it becomes much easier to valorize these materials through biorefining approaches.

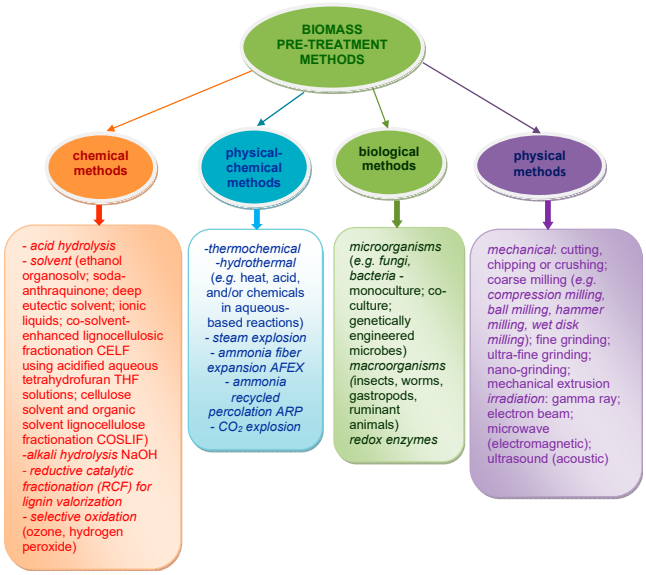


Figure 1. Schematic representation of strategies used for biomass pre-treatment.

As can be observed, the methods usually employed for biomass or cellulose substrates pre-treatment include chemical and physical (mainly mechanical), physical–chemical, and biological approaches. Various combinations of methods can be effectively applied for a facile interaction of biomass polymers with catalysts or other reagents in a further treatment stage [31–35]. For example, the treatment can lead to enhanced accessibility of enzymes and/or chemicals to polysaccharide-type components (cellulose and hemicelluloses), as well as their subsequent improved degradability [36].

In the case of native cellulose, known as cellulose I, a mixture of variable ratios of two crystalline allomorphs, Iα and Iβ, is present, one form being dominant in cellulose from bacteria and algae (Iα), while the other is dominant in cellulose from higher plants (Iβ) [37–39]. When cellulose I is subjected to chemical and thermal treatments, it is converted into other cellulose polymorphs (namely cellulose II, III, and IV), which present different crystal unit cells [40,41]. Both ordered (crystalline) and non-ordered (amorphous) regions are present concomitantly in the cellulose substrates. Additionally, the occurrence of the strong network created by intra- and intermolecular hydrogen bonds [42] impedes the easy access of different reagents to the cellulose substrates. Further, the lower reactivity of cellulose towards such reagents is closely related to and determined by its crystalline structure, which can rule out water access nearly totally [43]. In this context, the less ordered domains are more susceptible to react first and fast under various treatment conditions than the ordered domains. Thus, the decrease of crystallinity represents a prerequisite for a better reactivity of cellulose towards reagents, including enzymes, as well as for further improved degradability [32,35].

Recent reports on cellulose saccharification have emphasized the significant influence of pre-treatments on the process yield [31,32,44] and enabled a comprehensive database as well as a wide panel for comparison. Efficient saccharification of cellulose from different renewable sources to glucose is very useful when considering the production of energy and chemicals. Saccharification of cellulose substrates in aqueous enzyme solutions is characterized by a reduced rate, cellulose being a semi-crystalline biopolymer insoluble in water. The significant crystalline part of cellulose structure makes different substrates consisting of it less accessible to hydrolytic enzymes of cellulase type. The pre-treatment of cellulose-based materials improves their subsequent enzymatic catalysis by changing the cellulose crystallinity by modification of the allomorphic form of cellulose [45–47]. The enhanced biomass hydrolysis is mostly clear and related to the conversion of cellulose crystal

structure from the cellulose I form, highly crystalline, to the cellulose II crystal phase with reduced crystallinity [47]. Thus, this approach may represent a better alternative and more feasible way to enhance the rate of the subsequent enzymatic catalysis of cellulose materials when it is required. Total biodegradation of cellulose is a natural process, catalyzed by cellulases or cellulolytic microorganisms, that releases organic carbon as gas. There are specific types of enzymes (namely cellulases such as endocellulases, exocellulases, and β-glucosidases) involved in the complete saccharification of crystalline cellulose under enzymatic conditions [31,48,49].

The cellulase activity is usually measured using insoluble sources, including pure cellulose substrates such as Whatman No. 1 filter paper, cotton linter, microcrystalline cellulose, bacterial cellulose, and algal cellulose, as well as cellulose-containing substrates such as dyed cellulose, α-cellulose, and pre-treated lignocellulose [31,50,51]. Reduced saccharification efficiency is noticed in samples of pure cellulose materials, Avicel, and cotton fibers in relation to their high degree of crystallinity [52].

Usually, chemical and/or physical treatments are applied to lignocellulose materials in order to disrupt or weaken the strong bonds present between their polymer components, namely cellulose, lignin, and hemicelluloses. In effect, an easier degradation process occurs along with the conversion of these materials into useful biofuel intermediates. A comprehensive overview of applications and the development of a new class of solvents based on ionic liquids (ILs) systems for biomass pre-treatment, and cellulose dissolution strategies with a focus on environmental impact, as well as advantageous tunable properties of cellulosic materials resulted from their sustainable valorization processes were previously presented [53].

Therefore, the preliminary methodologies aiming to intensify the cellulose availability towards the enzyme attack are essential for the hydrolysis process of this polysaccharide consisting of β(1→4)-linked D-glucose units [31,54–57]. A modern pre-treatment method of cellulose substrates involves the use of ionic liquids (ILs), a new class of cellulose-dissolving solvents [53,58,59] and new reaction media for biocatalysis [31,60], highly effective as media for the enzymatic reactions of these polysaccharides [31,61–65]. The main effects on the cellulose substrates during pre-treatment with ionic liquids are represented mostly by changing, in a positive manner, their accessibility to enzymatic attack [66,67]. These changes may be expressed through:

(a) removal of hemicellulose and lignin;
(b) partial depolymerization of cellulose;
(c) crystallinity transition from cellulose I to cellulose II allomorph.

Ionic liquids seem to be easier to penetrate in biomass-derived cellulose material samples than Avicel samples, which are highly crystallized pure cellulose materials [68] with positive effects upon following enzymatic saccharification.

Cellulose substrates used in different studies on the influence of ILs pre-treatment on the enzymatic saccharification have included industrial softwood pulp [31], corn stover [44,69,70], rice straw [64,71], wheat straw [72], kenaf [73], switchgrass [63,74–76], bagasse [77,78], wood species such as poplar [76,79] and eucalyptus [77,80,81], and cellulose-enriched substrates, namely *Asclepias syriaca* seed floss and poplar seed floss [54–56].

Crystallinity changes during the pre-treatment with ILs include noteworthy conversion of cellulose I into cellulose II allomorph, as well as a consequent decrease of total crystallinity in cellulose substrates [61,82–86]. Mild treatment of lignocellulose materials using diluted solutions of ILs [87–89] results in the removal of hemicelluloses. ILs can be also employed in the selective fractionation of lignin–carbohydrate complexes by the cleavage of bonds that are the most susceptible to this type of processing [74,90]. Enhanced dissolution of polysaccharides, mainly those that are not bonded to lignin or have fewer

lignin bonds, can be achieved in the presence of suitable catalysts [91]. The dissolution of the supramolecular network formed in wood by the three biopolymers (namely cellulose, lignin, and hemicelluloses) through complex physical and chemical bonds is also possible [92–94]. The complete dissolution of both hardwoods and softwoods can be achieved by reducing the particle size of wood samples, but it is limited in the presence of water.

Efficient enzymatic hydrolysis of cellulose substrates is closely related to the decrease in the degree of polymerization of cellulose [48], which has been observed during pre-treatments with ILs [78,84]. The authors' previous studies [54–56] evidenced that pre-treatment with ILs modified the crystalline ordered structure of cellulose substrates (namely *Asclepias syriaca* seeds floss and poplar seed floss) with a positive impact on the enzymatic hydrolysis rates by increasing the accessibility of crystalline fraction of cellulose. A significant degradation process of both materials by pre-treatment with 1-ethyl-3-methyl-imidazolium-tetrachloroaluminate [EMIM]Cl-$AlCl_3$ was evidenced [56]. This process was caused by the increased acidity of the reaction medium which contributed to the enhanced depolymerization of cellulose and hemicelluloses by the hydrolysis down to smaller fractions.

Changes occurring in the ordered crystalline structure of cellulose materials offered the possibility to enhance the enzymatic saccharification, expressed as the releasing rate of reducing sugars and the hydrolysis yield. In general, the dissolution in ILs of natural polymers originating from cellulose materials can be an environmentally friendly alternative to conventional pre-treatment methods. Furthermore, this good dissolution in ionic liquid solvents such as [BMIM]Cl] can be further valorized as a successful chemistry strategy for the preparation of different cellulose derivatives [95].

Because the solvating power of ILs is usually impaired by the presence of water, a novel ionic liquid proactive in an aqueous medium and able to contribute to both the deconstruction and dissolution of lignocellulosic materials has been designed and tested as an effective, low-cost, and more fluid solvent. Consequently, an improved processability of the biomass resulted. Illustratively, the combination of [BMIM]Cl with lithium chloride, in the presence of water, improved up to a significant extent the solvating ability of this IL for the bamboo substrate [96].

3. FT-IR Spectroscopy and X-Ray Diffraction—Useful Methods for Evidencing the Crystalline Structure of Cellulose in Different Substrates

Biomass can represent a real problem when it is investigated using different characterization techniques, since it is a heterogeneous multi-component polymer material with softness, absorbent, and non-conductive properties. Furthermore, its biological conversion is strongly related to and impacted by its characteristics, both physical and chemical [48,97], such as the ratio of the chemical components, namely cellulose, lignin, and hemicellulose, as well as surface area, porosity, particle size, and wettability. All of these factors represent the macro-accessibility of the material, and last but not least, cellulose features (type, chain length/degree of polymerization, and the most important feature, crystallinity), which constitute the micro-accessibility [98].

The relative amount of crystalline part in cellulose substrates, namely the crystallinity index CI, is usually evaluated by the means of different investigation methods [99–105], including Fourier transform infrared spectroscopy (FT-IR), wide-angle X-ray diffraction (WAXD or XRD), solid-state ^{13}C nuclear magnetic resonance spectroscopy, solid-state ^{13}C cross-polarization magic angle spinning nuclear magnetic resonance spectroscopy (^{13}C CP MAS NMR), and FT Raman spectroscopy, as well as by the relatively new sum frequency generation (SFG) vibration spectroscopy technique [106–108]. A relatively new method of qualitative and quantitative assessment of changes in the crystalline structure of cellulose

in cotton fibers that occurs after the alkali treatment (NaOH) is represented by probing samples with a series of cellulose-directed binding modules (CBMs), and it was used in association with the FT-IR and XRD methods. This investigation does not change the crystallinity of the cellulose fiber during sample preparation as occurs when using XRD investigation, and it does not evaluate a bulk change in the sample as observed when employing the ATR-FTIR method. Its main advantage is its increased sensitivity, allowing at the same time the spatial analysis and mapping of the surface of individual cotton fibers for the occurred crystallinity changes. All techniques provide, in a common manner, both the relative crystallinity values and the tendency in crystallinity evolution. For example, cotton linter, known as an almost fully crystalline structure, yields the highest CI according to the different methods presented. There is no applicable and absolute technique for estimating the crystallinity value and investigating the cellulose structure, thus the best approach for calculating CI is to combine different techniques [109–111].

Determination of the crystallinity index using FT-IR spectroscopy is the simplest method, and it is based on the measurement of relative peak heights or areas [100,112,113], and such results are usually compared with those from XRD and/or NMR investigations. These spectra provide only relative values due to the presence of both crystalline and amorphous regions in substrates under investigation, considering the simultaneous presence of medium-ordered paracrystalline layers on the outer surface of crystalline cellulose [13].

The absorbance peaks at 1430 and 897 cm^{-1} are highly sensitive to the crystal structure of cellulose in lignocellulosic materials and can be used to study the type of crystalline cellulose and the crystallinity changes because the spectrum of crystalline cellulose I differs clearly from that of cellulose II and amorphous cellulose (e.g., when a significant amount of cellulose I is present in cellulose materials, the band is shifted toward 1430 cm^{-1}, the cellulose II and amorphous cellulose content being reduced). Thus, the absorbance ratio A1430/A897, which is known as the crystallinity index [114,115] or lateral order index (LOI), can be effectively used to indicate the cellulose I fraction in the substrate structure [116].

Another two infrared ratios that are closely related to the crystal system and the degree of intermolecular regularity in cellulose materials, and that are useful to evaluate the qualitative changes in crystallinity in cellulose, can be calculated as (1) A1372/A2900, which is known as the total crystallinity index (TCI) [117] and (2) A3308/A1330, known as hydrogen bond intensity (HBI) [116], respectively.

Generally, as HBI represents the hydrogen bonding between certain hydroxyl groups in cellulose, its increase means that crystallinity has decreased, which is typical for the conversion of cellulose I to cellulose II [118]. A higher value for crystallinity indexes, namely TCI and LOI, indicates that the substrate has an ordered structure, given its high content of crystalline cellulose, which can be partially transformed into amorphous cellulose through, for instance, treatments with ILs [75]. Some exemplifications from our previous studies will be presented in the next section.

The XRD method evidences in the resulting diffractograms relatively sharp and strong reflections attributed to the crystalline part of cellulose and broader signals characteristic to the non-crystalline part. The peak height method [99] is an empirical evaluation of the crystallinity index (CrI) calculated as the ratio of the intensity of the crystalline signal (I002-IAM) and the total intensity (I002) according to the following equation,

$$CrI\ [\%] = [(I_{_002} - I_{_AM})/I_{_002}] \times 100 \quad (1)$$

where I_{002} represents the maximum intensity of the signal corresponding to the (002) plane in the cellulose sample at a 2θ angle between 22° and 24° and I_{AM} is the intensity of the amorphous signal at a 2θ angle of about 18° corresponding to the minimum between (002) and (101) plane signals. The latter can be shifted to a higher value, ~19.5° for an

Avicel cellulose substrate for example [119], which evidenced the major drawback of this analytical method.

A previous article presented theoretical and experimental advances for the accurate ascertainment of the crystallinity of cellulose I materials using X-ray diffraction investigations [120]. Usually, the cellulose I form must be separated from the initial cellulose-based material, which also contains the cellulose II form, namely the amorphous cellulose. The crystallinity index value thus obtained is for qualitative evaluation only. Many investigations focused on a comparison of crystallinity index values in cellulose materials by means of diffraction and spectroscopy [102,103,121,122]. One study [102] evidenced a significant range of variation of the crystallinity index related to the methods used for its evaluation, applied for the same commercial microcrystalline cellulose (Avicel PH-101). The value ranged from 57% (from the NMR method) to 92% (from the XRD peak height method).

Furthermore, cellulose materials are seldom pure cellulose I. They also comprise other polymers (lignin and hemicelluloses), compounds (extractives and minerals), and last but not least, water that is linked chemically and/or physically to the substrate. All these components contribute to a large extent to the scattering intensity, in such cases requiring a correction defined on a dry basis cellulose material for an accurate determination of crystallinity index by XRD. Consistent CrI values can be obtained using multivariate statistical analysis applied to XRD spectra [121].

The same solid-state characterization methods (FT-IR and XRD) can be also successfully employed for the investigation of surface changes in wood samples before and after impregnation with natural-based products (vegetable oils, beeswax), as well as under biodegradation conditions in soil burial tests [123].

4. Crystallinity Changes in Cellulose Substrates Evidenced by FT-IR Spectroscopy

FT-IR spectroscopy represents an effective useful method of investigation when it comes to substantiating the structural changes in cellulose substrates [124].

One of the authors' previous studies [125] focused on the interaction of cellulose and lignocellulose substrates (namely microcrystalline cellulose MCC-Avicel, beech wood sawdust BWS, and cellulose separated from beech wood BWC) with the ionic liquid 1-ethyl-3-methyl-imidazolium chloride ([EMIM]Cl), and their structural features before and after regeneration from solution (MCC_r, BWS_r, BWC_r) investigated by the means of FT-IR spectroscopy and X-ray diffraction. The FT-IR spectra (Figures 2–4) showed characteristic cellulose peaks, as follows: the absorption band near 1160 cm^{-1} provides evidence of the anti-symmetric bridge stretching of the C-O-C groups, while the absorption band near 1318 cm^{-1} can be ascribed to the CH_2 wagging vibrations in cellulose and hemicelluloses; the absorption band noticed at 1635 to 1640 cm^{-1}, attributed to the absorbed water-bending vibrations, significantly decreased for cellulose substrates in the presence of IL [125]. As expected, the crystalline well-ordered phase and the degree of intermolecular regularity were noticeably influenced by the presence of IL, which promoted significant changes in the substrate structure. Some infrared ratios closely related to the crystal system and the degree of intermolecular regularity in cellulose materials as presented above were calculated from FT-IR spectra and are presented in Table 1.

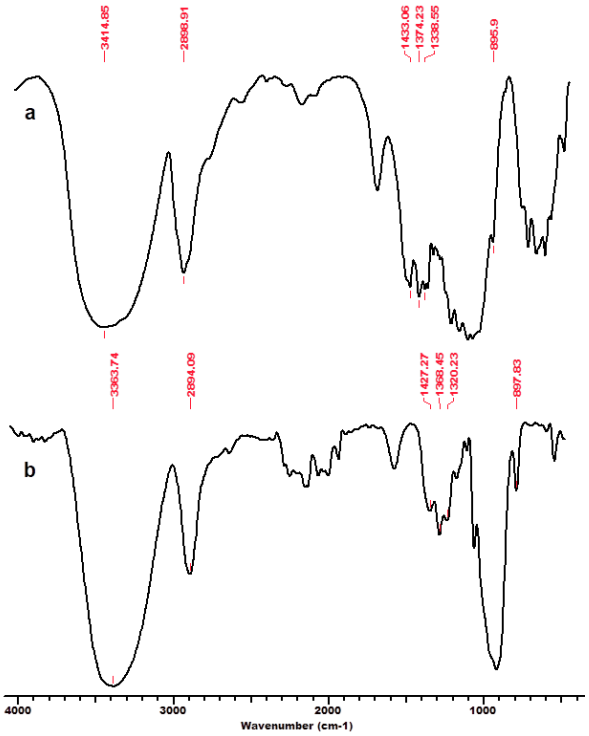


Figure 2. FT-IR spectra for microcrystalline cellulose MCC, initial (**a**) and after regeneration process in ionic liquid [EMIM]Cl–MCC_r (**b**). Permission to re-draw and reuse figures obtained from Romanian Academy, copyright holder [125].

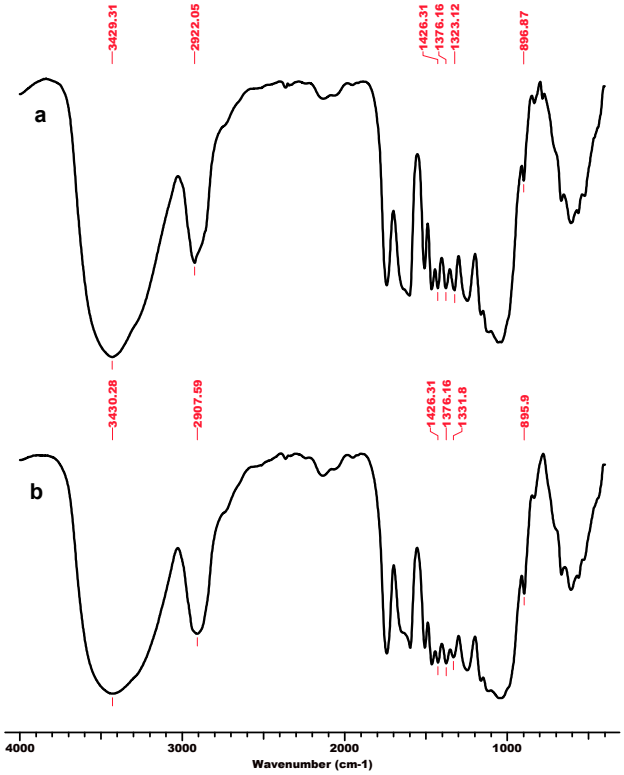


Figure 3. FT-IR spectra for beech wood sawdust BWS, initial (**a**) and after regeneration process in ionic liquid [EMIM]Cl–BWS_r (**b**). Permission to re-drawn and reuse figures obtained from Romanian Academy, copyright holder [125].

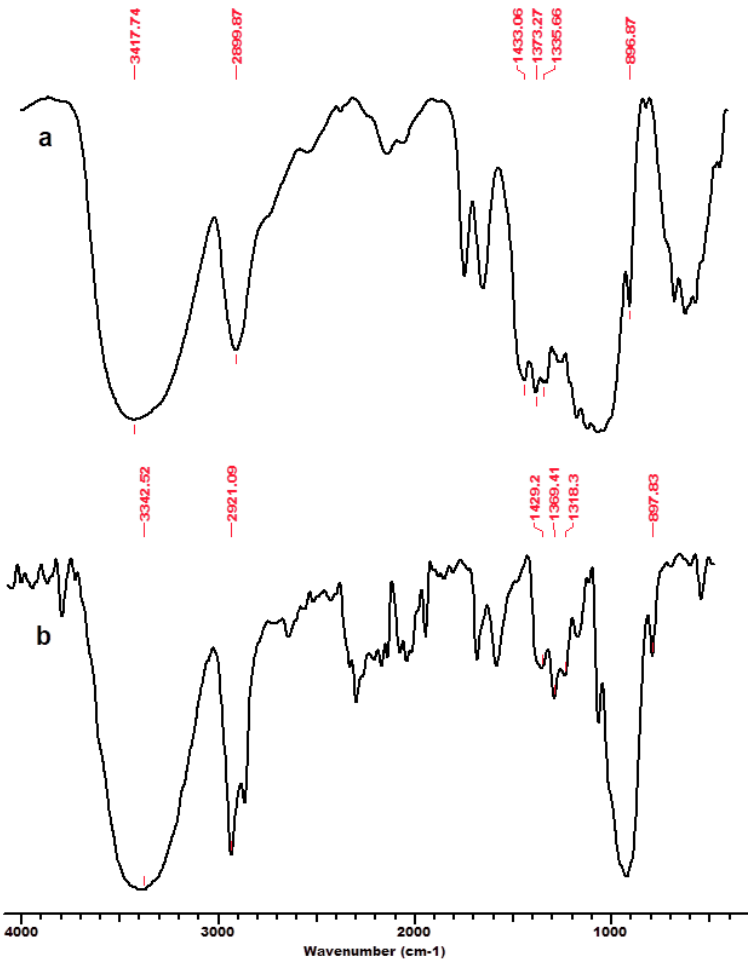


Figure 4. FT-IR spectra for beech wood cellulose BWC, initial (**a**) and after regeneration process in ionic liquid [EMIM]Cl–BWC_r (**b**). Permission to re-draw and reuse figures obtained from Romanian Academy, copyright holder [125].

Table 1. Crystallinity indexes and hydrogen bonding intensity of some cellulose substrates, initial and after regeneration in ionic liquid [EMIM]Cl.

Cellulose Substrate	TCI (A_{1372}/A_{2900})	LOI (A_{1430}/A_{897})	HBI (A_{3308}/A_{1330})
MCC initial	1.269	1.514	1.502
MCC_r	0.662	1.332	5.555
BS initial	1.243	2.845	1.993
BWS_r	1.164	2.061	1.560
BWC initial	1.369	1.738	0.676
BWC_r	0.297	1.106	5.750

MCC—microcrystalline cellulose; BWS—beech wood sawdust; BWC—cellulose from beech wood; Permission to re-write tabular data obtained from Romanian Academy, copyright holder [125].

An interesting feature is related to the peak at 2900 cm^{-1} attributed to the C-H and CH_2 stretching, which remained unaffected by changes in crystallinity (related to changes in hydrogen bond networks that were disrupted) caused by the considered treatments (ionic liquid and subsequent regeneration) [117]. A high index value indicated that the cellulose material has a significant crystalline domain with a highly ordered structure. The TCI values significantly decreased for substrates comprising dominantly cellulose,

namely MCC and BWC, after treatment with IL and the regeneration process (Table 1). This indicates that a part of the crystalline structure of cellulose was transformed into its amorphous allomorphs [125]. Thus, the structural changes caused by the interaction of cellulose substrates with IL were due to the altered crystalline phase and decreased degree of intermolecular regularity.

Other studies [45–47] also evidenced that the modification of the cellulose crystalline structure by pretreatments (e.g., ionic liquid, heat, alkaline, ethylenediamine, or a combination) influenced in a positive manner the enzymatic hydrolysis of cellulose mainly through transformation of cellulose allomorph and a decrease in crystallinity. In the case of lignocellulose substrates, lignin degradation can occur under appropriate, usually combined, pre-treatment conditions (e.g., heat and ethylenediamine). Cellulose treated with IL ([BMIM]Cl) was very close to amorphous cellulose having a crystallinity index value of 20% [45].

Other investigations [54–56] have considered the behavior of some cellulose-enriched materials, namely *Asclepias syriaca* seed floss (ASF) and poplar seed floss (PSF), treated with different ionic liquids ILs with or with no further enzymatic hydrolysis. Structural changes that occurred in cellulose substrates can be evidenced by FT-IR spectroscopy with the calculation of the index values characteristic to the crystallinity evolution under specified conditions, data presented in Table 2.

Table 2. Crystallinity indexes and hydrogen bonding intensity of some cellulose substrates, initially and after dissolution in different ionic liquids with or without further enzymatic hydrolysis.

Cellulose Substrate and Treatment	TCI (A_{1372}/A_{2900})	LOI (A_{1430}/A_{897})	HBI (A_{3308}/A_{1330})
ASF	0.84	2.41	5.35
ASF(EH)	0.96	1.72	4.38
ASF-IL1	0.75	2.15	4.80
ASF-IL1(EH)	0.98	1.14	4.73
ASF-IL2(EH)	1.04	1.40	4.10
ASF-IL3(EH)	1.06	1.19	3.86
ASF-IL4	0.82	2.06	3.90
ASF-IL4(EH)	0.79	2.95	3.52
PSF	0.52	2.72	4.42
PSF(EH)	0.60	1.97	3.95
PSF-IL1	0.73	2.41	4.38
PSF-IL1(EH)	0.66	1.85	3.90
PSF-IL2(EH)	0.56	1.62	3.92
PSF-IL3(EH)	0.71	1.60	3.91
PSF-IL4	0.79	2.35	4.37
PSF-IL4(EH)	0.71	2.65	4.23

ASF—*Asclepias syriaca* seed floss; PSF—poplar seed floss; EH—enzymatic hydrolysis with cellulase; IL1—1-buthyl-3-methyl imidazolium chloride [BMIM]Cl; IL2—1-ethyl-3-methyl-imidazolium chloride [EMIM]Cl; IL3—1-butyl-4-methyl pyridinium chloride [BMP]Cl; IL4—1-ethyl-3-methyl imidazolium aluminium tetrachloride [EMIM]$AlCl_4$ (written by authors from the data presented in [54–56]).

The TCI value for cellulose substrates showed an increase after treatment using ILs, with or without further enzymatic hydrolysis, while LOI and HBI values were lower under the above-mentioned treatment conditions as compared to the raw materials. The crys-

tallinity changes that occurred were closely related to the different chemical structures of ILs used for treatment. A significant gain when using ILs for the dissolution of cellulose substrates is represented by their positive effects on the further enzymatic hydrolysis, expressed by the increased corresponding rates, as exemplified below (see Figures 5–7, which were drawn by the authors). This feature is closely related to the increasing fraction of amorphous cellulose during the enzymatic treatment on account of the decreasing crystalline cellulose fraction. Some differences are noticed when 1-ethyl-3-methyl imidazolium aluminium tetrachloride [EMIM]$AlCl_4$ is used for the dissolution of cellulose substrates, because of the increased acidity of the reaction medium which contributed to the enhanced depolymerization of polysaccharides components (cellulose and hemicelluloses) by the hydrolysis down to smaller fractions (in other words, a more intense degradation process of the cellulose substrates occurred). Its effect is less pronounced in comparison with 1-buthyl-3-methyl imidazolium chloride [BMIM]Cl, but important also are the different structural features of cellulose substrates (ASF is composed of 54.9% cellulose, 8.0% hemicelluloses, 19.3% lignin, and 0.9% ash, while PSF is composed of 62.07% cellulose, 17.04% lignin, and 2.5% ash [56]). As one can observe from Table 2, the nature of the raw cellulose materials (mainly the degree of polymerization and crystallinity of cellulose in relation to the kind of cellulose substrate: pure cellulose, cellulose-rich materials, or lignocellulose) influences, to a large extent, their behavior under different treatment conditions, mainly when using ILs prior to the enzymatic saccharification.

It is also very important to take into consideration both the inherent presence of impurities and treatment parameters (reaction time, temperature, and initial concentration of cellulose materials in ILs), which are essential for an efficient treatment of cellulose materials to overcome their inherent inertness, in relation with further effective strategies for their valorization through biorefinery approaches.

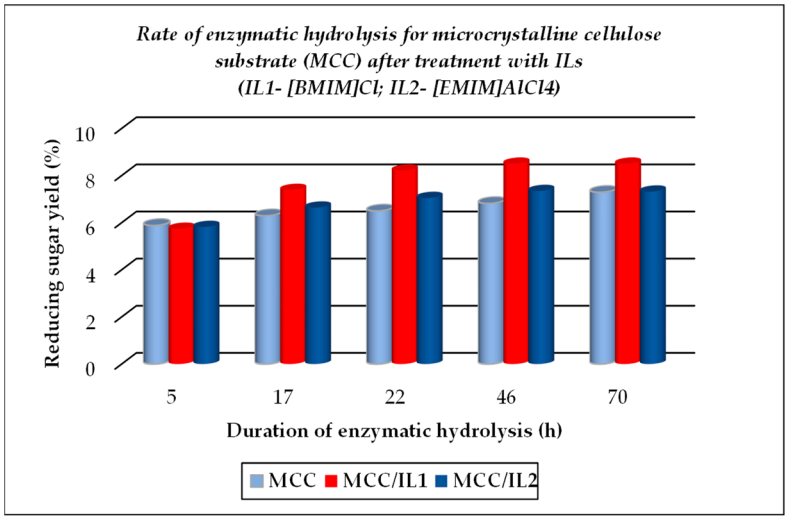


Figure 5. Evolution of enzymatic hydrolysis, as rate, for microcrystalline cellulose (MCC), initial and after treatment with ionic liquids ILs.

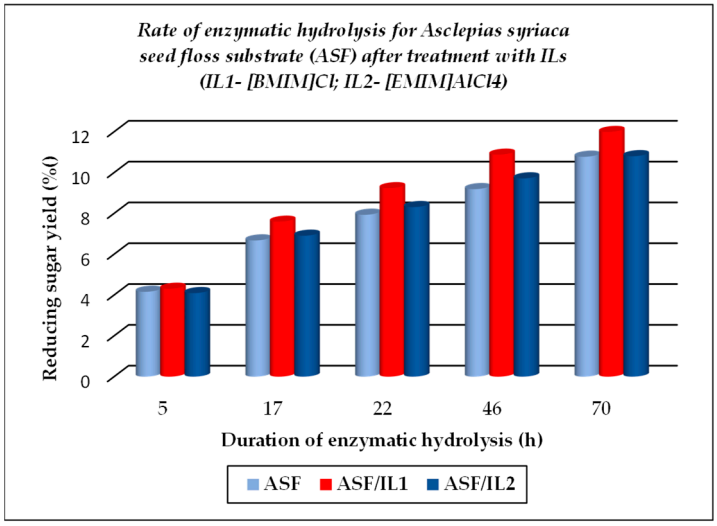


Figure 6. Evolution of enzymatic hydrolysis, as rate, for *Asclepias syriaca* seed floss (ASF), initial and after treatment with ionic liquids ILs.

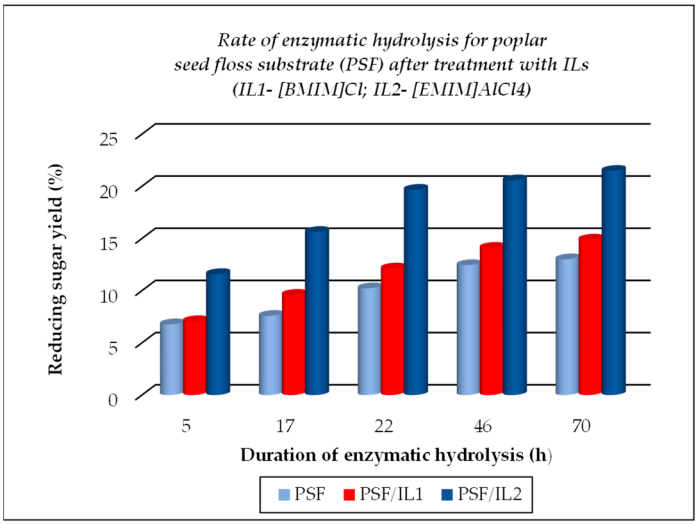


Figure 7. Evolution of enzymatic hydrolysis, as rate, for poplar seed floss (PSF), initial and after treatment with ionic liquids ILs.

5. Crystallinity Changes in Cellulose Substrates Evidenced by X-Ray Diffraction

General Considerations

The reactivity of cellulose intended for superior valorization strongly depends on its purity and accessibility: the more available the cellulose glycosidic ether bonds (β-1,4 glycosidic bonds), the more effective its conversion [32,126]. The accessibility of cellulose strongly limits the effectiveness of treatments, and various factors influence it, such as the content in lignin and hemicelluloses, porosity, specific surface area of particles, degree of polymerization, and crystallinity [127]. It has been shown that the amorphous cellulose is more susceptible to hydrolysis under mild acidic conditions (e.g., manufacture of micro-crystalline cellulose Avicel), in contrast to the crystalline cellulose which is highly ordered due to the intermolecular hydrogen bonds and van der Waals interactions. Therefore, it is necessary to reduce the cellulose crystallinity in order to achieve enhanced accessibility and, hence, a higher degree of modification. Thus, mechanical (wet or dry), chemical (water, organic reagents and solvents, swelling agents, ILs, etc.), physical (radiative, microwave, etc.), or even enzyme treatments applied to raw or processed biomass yielded in cellulose

and cellulosic materials with reduced crystallinity and increased responsivity to further procedures [128–132].

Evaluation of cellulose crystallinity by XRD began in the first decade of the 20th century, and the method is still employed to compare the diffractograms for crystalline and amorphous fractions [133–135]. Thus, the crystalline cellulose is highly reflective, which yields sharp peaks, while the signals assigned to amorphous cellulose are wider and have lower intensity [32,136]. Several methods have been developed, such as weighing the pieces of paper that correspond to the crystalline and amorphous sections of the graphs (the Hermans and Weidinger method) [137,138] and comparison between the peak intensity of the crystalline fraction and the total intensity without the background signal (the Segal method) [99]. However, such methods are empirical and there are errors due to the hypotheses considered; even more, they do not take into consideration that crystallites of small size give broad signals, but their contribution to the overall intensity is poor. Therefore, significant differences occurred between the crystallinity values when calculated by subtracting the amorphous contribution at $2\theta = 21^\circ$ and 18° (assigned 21-WAXS and 18-WAXS or Segal method, respectively).

The XRD amorphous subtraction method, namely Ruland and Vonk [139,140], measures the crystallinity by subtracting the contribution of the amorphous fraction from XRD graphs. Results are compared to an amorphous standard, which has to be appropriate and according to the amorphous fraction in the sample. This method allows comparison between cellulosic samples of various origins, raw and treated, and xylan and lignin [141]. Thus, it was possible to conclude that amorphous cellulose should be employed as the standard for cellulose in order to enhance the accuracy of the measurements of its crystallinity. On the other hand, a mixture of xylan and lignin is a more appropriate standard for XRD measurements of hardwood prior to and after treatments.

By using fitting functions such as Gauss [142] and Lorentz [143,144], a more precise deconvolution is possible, which can lead to more accurate conclusions. Even more, some typical assumptions had to be changed as the number of crystalline peaks considered for calculations varied, the fitting software advanced, selected parameters were different, and even the crystallites' size, type, geometry, and orientation had to be reassessed [145].

Taking into consideration the features of each XRD method, it is obvious that all have limitations and none of them allows quantitative measurement of crystallinity. Still, it can be reasonably agreed that two methods, namely the XRD peak height and XRD amorphous subtraction, afford reproducible results with good accuracy.

6. XRD Evaluation of Structural Changes of Cellulose Substrates After Their Modification

Surface modification of biomass comprises various treatments (physical, chemical, and enzymatic) aimed at improving significantly the accessibility and reactivity of cellulose. This is achieved by the disruption of the supramolecular architecture in all cellulose substrates, whether biomass (when other components, such as lignin, hemicelluloses, and waxes are also exposed) or pure cellulose. Purity, particle size, degree of polymerization, and crystallinity are modified after the treatment.

6.1. Physical Treatments

Mechanical methods of modification of biomass, namely ball milling (wet or dry), mix milling, and reactive milling, may cause severe reduction in particle size and crystallinity [146–148] without a significant increase in cellulose purity. However, these effects are important when the biomass is further processed in biorefineries for chemical production [149]. It has been demonstrated that by employing pretreatments in various

combinations, it was possible to obtain high conversion yields and, therefore, they are preferred. Thus, milling was used in combination with either physical (such as irradiation, microwaves, sonication, or even electron beams) or chemical treatments (i.e., ball milling in the presence of water, acids, or acidic clays) [34,150,151], or the addition of solvents, enzymes, and other reagents [152]. However, such approaches have worked only at the laboratory scale; most of them are difficult to transfer to the industrial scale due mainly to the expensive, energy-intensive equipment [32]. It was also evidenced for microcrystalline cellulose that mechanical treatments influenced the crystallinity, degree of polymerization, and particle size, depending on the frequency of milling and duration of the procedure, up to certain values. Thus, after milling at 10 Hz for 4 h, the values of the particle size reached a plateau and no further decrease was noticed, a fact that may be explained by considering the secondary agglomeration of particles during applying prolonged milling [153]. Nevertheless, the effect of crystallinity of cellulosic substrates on the mechanical refining-assisted alkaline pretreatment, eventually followed by hydrolysis (i.e., enzymatic hydrolysis) has not been studied extensively enough, so experimental or multivariate analysis data are scarce [154]. Thus, it has been demonstrated that a cellulosic substrate with a high crystallinity index is difficult to submit to enzymatic saccharification efficiently, as it resists refining. However, samples that have been previously treated (mechanical and alkaline pretreatments) showed reduced crystallinity and improved availability for the subsequent enzymatic hydrolysis.

On the other hand, the lignin content and the buffering character of cellulose may also strongly influence the crystallinity reduction, so advanced purification and delignification of biomass prior to treatment should be addressed. Low acidic activated carbons were also used in mix ball-milling due to their efficiency: the rate constant was 13 times higher than for ball milling without them, confirming thus their catalytic effect. The low crystallinity index values determined by the means of ^{13}C-CP/MAS NMR and XRD (peak height method) validated the high yield of this solid–solid reaction [155]. Furthermore, these activated carbons can be easily regenerated even when loaded with solid residues (lignin) [156]. Irradiation has been shown to be another effective pretreatment of biomass in terms of decomposition and depolymerization of its constitutive natural polymers. Whether it employs gamma rays [157], electron beams [158], microwaves [159,160], or ultrasound [161] irradiation, the process increases the accessibility of cellulose, followed by a reduction of the particle size and a more intense mass transfer, although the decrease in crystallinity may be of no consequence or, sometimes, the crystallinity may slightly increase due to the removal of amorphous cellulose, lignin, and hemicelluloses [162]. Despite its benefits, irradiation as a pretreatment has been applied in industry only at a limited scale because it requires expensive equipment and supplies, and it is a highly energy-consuming process.

Plasma treatments are relatively recent methods applied for cellulose substrates as dry procedures. Non-thermal atmospheric plasma (NTAP) treatment was used in order to increase the cellulose degradability by reducing its degree of polymerization (DP), as a precondition of a high-yield conversion. Thus, the DP of Avicel PH-105 microcrystalline cellulose was reduced from 200 to 120 by means of the NTAP treatment (11 kV, 2 kHz, 3 h), followed by the cellulose hydrolysis in the presence of the solid acid catalyst Amberlyst 35, at 150 °C, for 1 h [163]. As with irradiation, plasma treatments have some advantages (the use of dry gases, high efficiency at low temperatures, no solvent or catalyst, no subsequent purification process, selectivity, etc.) that can balance the associated drawbacks [164].

The hydrothermal treatment of biomass allows lignocellulose to interact with hot water or steam, which enables partial degradation along with the redistribution of lignin and hemicelluloses [165]. Several different processes occur and alter the crystallinity of the final products. Thus, the partial degradation of hemicelluloses yields organic acids with

small molecules (e.g., acetic acid) which, in turn, act as catalysts. The partial degradation of lignin favors reactions of depolymerization/recombination by means of some aryl-ether bonds cleaved under acidic catalytic conditions, with the formation of carbonium ions as intermediates [166,167]. At the same time, lignin may undergo melting processes due to the high temperature of the treatment, followed by redistribution upon cooling [168]. As a result, the material achieved a larger pore volume and the accessibility of cellulose increased, which had beneficial effects on the reduction of the degree of polymerization and crystallinity, respectively [169]. Additionally, aggregation phenomena were reported for cellulose under hydrothermal conditions [170,171]. At elevated temperatures and pressures, and considering the associated loss of lignin and other constitutive polymers, cellulose–cellulose interactions tend to become widespread, leading to the formation of larger crystallites with significantly increased lateral dimensions. Water molecules linked by hydrogen bonds to the amorphous regions of biomass polymers expand under hydrothermal conditions and disrupt the ordered supramolecular structure of the crystalline regions of the substrate, thus reducing the crystallinity and exposing cellulose, enhancing its accessibility. This type of treatment has disadvantages as well, the main being the formation of by-products (furfural and hydroxymethyl-furfural, phenols, etc.), which are able to severely limit the conversion processes [32].

6.2. Chemical Treatments

Acid and alkaline treatments have been also considered for the removal of lignin and hemicelluloses [172,173]. Even more, these treatments have been applied for the production of monomeric sugars directly from cellulose and hemicelluloses [174].

Generally, acidic treatments can be performed on biomass in diluted or concentrated solutions, at high or low temperatures, depending on the nature of the substrate, the envisaged end products, or the severity of the process. Illustrative examples of inorganic acids are HCl and H_2SO_4 as the most widely used, but other mineral acids have been considered too, such as HF, HNO_3, H_3PO_4, and SO_2 [32]. For example, the use of H_3PO_4 as a pre-treatment proved to be highly effective under varying conditions. Thus, when the sample was immersed for 10 h in a concentrated solution of H_3PO_4 (85%), the XRD data indicated the conversion of cellulose I to cellulose II, which confirmed the decrease in the crystalline index; at the same time, the cellulose crystal width decreased by half; at the end of the treatment, the entire crystalline cellulose had been transformed into amorphous cellulose [175]. Under different conditions (conc. 85%, 50 °C, 40 min), H_3PO_4 caused a significant decrease in the crystallinity index of cellulose, from 85% down to 33% (evidenced by the means of XRD, the peak height method [176], due to cellulose swelling and moderate hydrolysis. Organic acids have been employed as well for acidic hydrolysis under specific conditions: maleic [177] and fumaric acid [178], oxalic acid [179], which is more selective than H_2SO_4 in the hydrolytic cleavage of β-1,4 glycosidic bonds; formic acid [180], acetic acid [181] and heteropolyacids [182].

Similar to other treatments, the advantages and drawbacks of acidic hydrolysis must be comparatively highlighted. Cellulose can swell or/and dissolve in the presence of concentrated inorganic acids; their use at low temperatures proved to be more energy efficient than the use of diluted acids at high temperatures. Organic acids, such as formic acid and acetic acid, can dissolve lignin when applied in concentrated solutions [183]. Strong acid treatments can also lead to the further degradation of reaction products (sugars are converted to furfural and hydroxymethylfurfural, organic acids, humic acids, and derivatives) [184]. Still, inorganic acids are highly corrosive and require large amounts of neutralizing agents, which makes them very difficult to recycle, while heteropolyacids can be removed by precipitation as insoluble cesium salts [185].

Another issue of interest is the effect of the crystallinity of cellulosic substrates on the rate of hydrolysis. In a comparative study, when amorphous carboxymethyl cellulose (CMC) and highly crystalline wood shavings were submitted to enzymatic hydrolysis, it was demonstrated that the reaction effectiveness was very low in the high crystalline areas of wood shavings and only their amorphous regions have undergone hydrolysis [186]. Following the same line, it has been demonstrated that highly crystalline CMC had low hygroscopicity and reduced susceptibility to undergo hydrolysis when used in pharmaceutical formulations. However, ground CMC with a decreased crystallinity index showed a pronounced propensity to water sorption and higher sensitivity to hydrolysis [187]. The explanation resides in the modification of the crystalline/amorphous ratio by grinding. The increased amount of amorphous CMC has a disordered supramolecular structure with many entanglements due to the increased number of hydrogen bonds which further favor the binding of water molecules. The lower the crystalline index and particle size after grinding, the higher the rate of water penetration.

Alkaline treatments aim at biomass delignification as a result of lignin removal (by breaking the ether bonds) and solubilization of hemicelluloses (via saponification of intermolecular ester bridges between lignin and hemicelluloses), yielding in an increased porosity and cellulose accessibility. Unlike hemicelluloses, cellulose is rather stable under alkaline conditions, although certain depolymerization processes occur along with the random cleavage of cellulose macromolecular chains and the formation of small molecules (e.g., lactic acids) that are able to undergo further processing [188]. Still, concentrated alkaline solutions (NaOH aq. sol. 8 to 20%) were reported to cause swelling and dissolution of the native cellulose I, but only cellulose II polymorph (the main features of the supramolecular structures of these cellulose polymorphs are illustrated in Figure 8) resulted upon recrystallization after neutralization (a process known as mercerization).

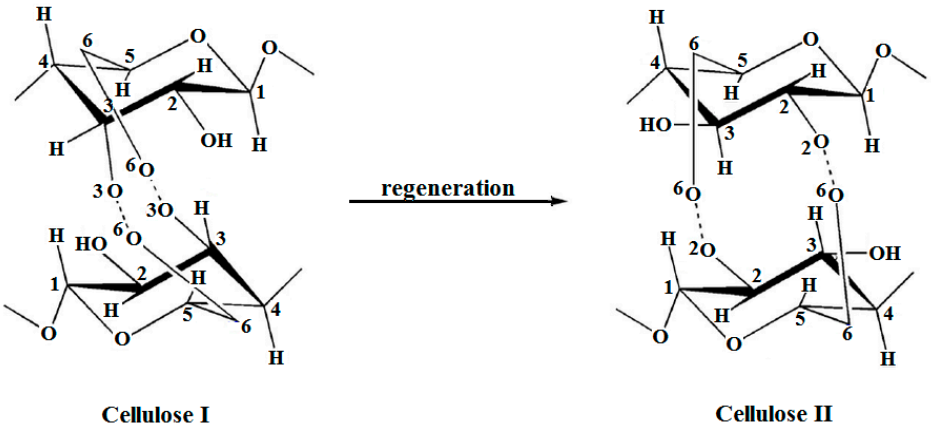


Figure 8. Cellulose I and II polymorphs—supramolecular structures.

Despite this partial recrystallization, the overall crystallinity of the material decreased notably. XRD proved to be very useful when it came to the discrimination of the polymorphic changes in cellulose originating from various species and the characterization of the corresponding crystallites [189,190]. Even more, advanced X-ray spectrometric methods and combined techniques allowed the calculation of the diffraction patterns, discrimination among different cellulose polymorphs, and assessment of crystal dimensions for both powders and fibers [135,191–193], or even enabled the characterization of materials with tailored properties obtained by altering the cellulose polymorphs [194].

Cellulose I and II undergo a swelling process in the presence of liquid ammonia due to the cleavage of the hydrogen bonds and the formation of a cellulose–ammonia complex [195]. The subsequential crystalline transition to cellulose III_I and III_{II} polymorphs

upon ammonia evaporation depended on the processing parameters (e.g., temperature). In a mixed alkaline treatment (medium of NaOH and NH_3 aq. sol.), cellulose from different sources (corn stover, Avicel, cotton) underwent a significant decrease in crystallinity. The study confirmed that cellulose I converted to cellulose II in the presence of NaOH (the regenerated cellulose II had a lower crystallinity index due to the antiparallel chain alignment), while the liquid ammonia treatment yielded in cellulose III_I allomorph (the crystallinity depended on the processing parameters) [196].

Ammonia fiber expansion (AFEX) treatment employs liquid ammonia in the presence or absence of water, and upon heating for various time intervals, in the range of 5 to 60 min, with no mass loss (dry-to-dry process), when both cleavage reactions (namely aminolysis and hydrolysis) of ester intermolecular bridges between lignin and hemicelluloses take place [197]. Other characteristics of this process are the very low amount of resulting furan-type products and the formation of numerous pores with dimensions varying from 10 nm up to 1000 nm; under anhydrous conditions, the decrease in cellulose crystallinity is significantly higher because the effect of ammonia is not hindered by water molecules [198]. Given that moisture limits the formation of cellulose III allomorph, a new procedure was developed and applied with good results, namely the extractive ammonia method (EA) [199,200]. Still, the treatment is yet under study as its drawbacks (high-pressure process, formation of toxic by-products, loss of catalysts, and disruptive side reactions) overcome the benefits.

Oxidation reactions, whether they were performed in the presence of specific reagents (such as H_2O_2, O_3, peracids, chlorite, and hypochlorite, etc.), in aqueous solution or alkaline (NaOH, ammonia) media, and in the presence of catalysts or enzymes, were successfully employed to reduce cellulose crystallinity of biomass from different sources (sugar cane bagasse, wood, corn stalk [32]).

Reductive catalytic fractionation (RCF) of biomass uses hydrogen or hydrogen transfer reagents in order to depolymerize and stabilize reactive intermediates in aqueous or non-aqueous organic solvents by hydrogenation or hydrogenolysis [201–205]. It may be considered a promising approach because it allows the lignin fractionation, along with the separation and valorization of hemicelluloses, but it had low effectiveness in terms of decrease of cellulose crystallinity, as confirmed by XRD studies (peak height method) performed on treated and raw eucalyptus cellulose [206]. Still, the pH of the reaction medium had some influence on the crystallinity of cellulose, as it decreased in an alkaline environment, but it remained unmodified under acidic conditions [207].

6.3. Solvolysis. Use of Ionic Liquids (ILs) for Cellulose Substrates

The organosolv fractionation was considered as well. Water and organic solvents can cause a significant swelling of the biomass since they penetrate the amorphous regions by hydrogen bond interactions and perturb the rigorous supramolecular structure of crystalline cellulose. As a result, lignin and hemicelluloses are solubilized and sometimes even degraded. The literature is abundant in studies that report on various solvents and the specific conditions (most organosolv systems evolve as autocatalytic processes at high temperatures) used for this type of treatment [32]. It is well known that the low solubility of cellulose in water is enabled by the hydrogen bonding and hydrophobic interactions so that strong intrinsic cohesion forces do not allow the disruption of the crystalline network. Therefore, a new generation of solvents was required, solvents able to access the cellulose macromolecular chains by physical intermolecular interactions (non-derivatizing solvents) or by labile, short-termed chemical interactions that evolve through ester-, ether-, or acetal-type intermediates (derivatizing solvents). Aside from the classic polar protic and aprotic solvents and mixtures of solvents, another group of solvents that can act in both ways

is represented by the ionic liquids (ILs) [90,208]. Such solvents have been shown to be effective in reducing the cellulose crystallinity. Thus, 1-allyl-3-methylimidazolium chloride (AmimCl) and 1-ethyl-3-methylimidazolium acetate (EmimAc) have been employed for cornhusk cellulose which presented a decreased crystallinity, from 59.6% to 48–49%, after regeneration from ILs [209]. 1-N-butyl-3-methylimidazoliumchloride ($[C4mim]^+Cl^-$) has been used to solubilize cellulose from filter paper and WAXD patterns confirmed that regenerated cellulose showed peaks characteristic of allomorph cellulose II, which has a reduced crystalline index, and their intensity was significantly diminished [210]. The most common cations and anions employed in IL formulations are presented in Figure 9.

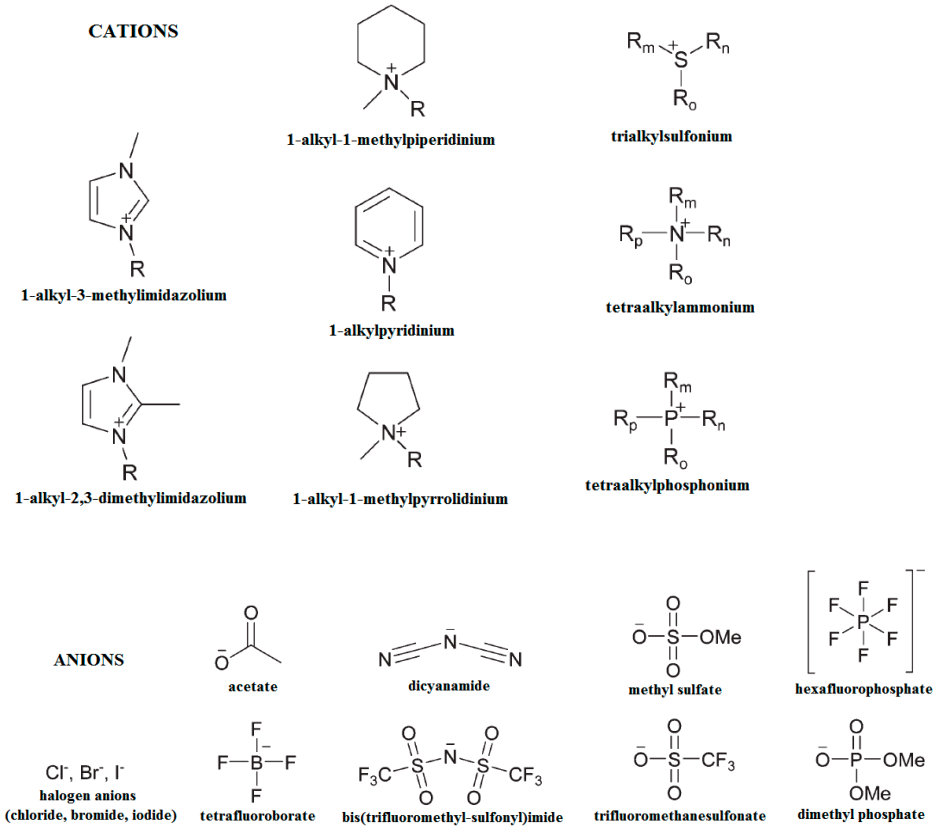


Figure 9. Selected cations and anions used in IL formulations.

ILs can act as both solvents and catalysts in the conversion of cellulose from biomass [209], although some of them, such as 1-ethyl-3-methylimidazolium acetate ([EMIM] OAc), are able to solubilize lignin as well [211]. ILs have been used as pre-treatments for the activation of cellulose prior to other procedures (e.g., enzymatic treatment or chemo-catalytic conversion) [53,212]. When biomass was treated with ILs, it was possible to recover and isolate the cellulose by precipitation using additionally an anti-solvent, such as alcohol or water [213]. The decrease in cellulose crystallinity subsequent to the ILs treatment has been substantiated by the XRD study of the transition of cellulose I to cellulose II, which showed a disrupted order and a diminished crystallinity [83].

Systematic experimental studies [214,215] indicated that [EMIM]OAc was the most effective IL in terms of cellulose dissolution, while [AMIM]Cl showed the highest efficiency in dissolving wood chips. A treatment with a solution of [EMIM][OAc] in water (50 to 80 wt%) at 160 °C produced cellulose with decreased crystallinity and enhanced digestibility, in correlation with the IL solution concentration, in so far as water may serve as co-solvent/anti-solvent, and designed IL-water mixtures can be efficient treatments for biomass of different origin.

In addition to the solubilization, cellulose with reduced crystallinity can be obtained by initiating scission reactions, resulting in cellulose depolymerization. Thus, when solid acid catalysts (such as p-toluene sulfonic acid or Amberlyst™ 15Dry) were added to the ILs, the degree of polymerization of the resulting cellulose was 10, after a 5 h treatment in [BMIM]Cl (1-butyl-3-methylimidazolium chloride), at 100 °C [216–219]. Various combinations of ILs and solid acid catalysts have been designed and tested. For example, [BMIM]Cl was successfully employed in the treatment of cellulose substrates in the presence of cation-exchange resins (Nafion NR50 [212] and Amberlyst 35 [163]) sulphated zirconia, and phosphoric acid-activated carbon [220]. Other solid acid catalysts have been employed as well. Thus, for the treatment of Avicel PH-101 microcrystalline cellulose with [BMIM]Cl at 180 °C, for 4 h, Norit CAP Super has been used in the presence of H-mordenite (Si/Al = 45) as an activated carbon acid scavenger to ensure high glucose yields [221]. Amberlyst 15 led to a highly increased yield of biomass saccharification (substantiated by the low amount of cellulase required) when added to the [BMIM]Cl treatment of switchgrass [222]. Conversion of cellulose I into cellulose II was evidenced by XRD for cellulose substrates treated with 1-N-butyl-3-methylimidazolium chloride or 1-allyl-3-methylimidazolium chloride as well [212]. ILs may be employed in the cellulose catalytic alcoholysis in order to augment the conversion of cellulose to glucose. The process is deployed in stages: the pre-treatment in the presence of 1-allyl-3-methylimidazolium chloride ([Amim]Cl), followed by the catalyzed alcoholysis (heteropolyacid H3PW12O40 as catalyst) with the formation of methyl glucosides (yield of 70.2 wt%) [223]. Another approach is the ILs-assisted selective dissolution of lignin from biomass (the Ionosolv process performed in the presence of [EMIM]OAc and [BMIM]Cl) when purified cellulose with slightly decreased crystallinity resulted after filtration [90]. XRD investigation may evidence the significant disruption of the crystalline structure of cellulose regenerated from ionic liquid solutions such as [EMIM]Cl, as shown for cellulose substrates coded as MCC_r, BWS_r, and BWC_r [125], indicated by the absence of the diffraction peaks characteristic to the well-ordered domains in the diffraction profiles (Figure 10).

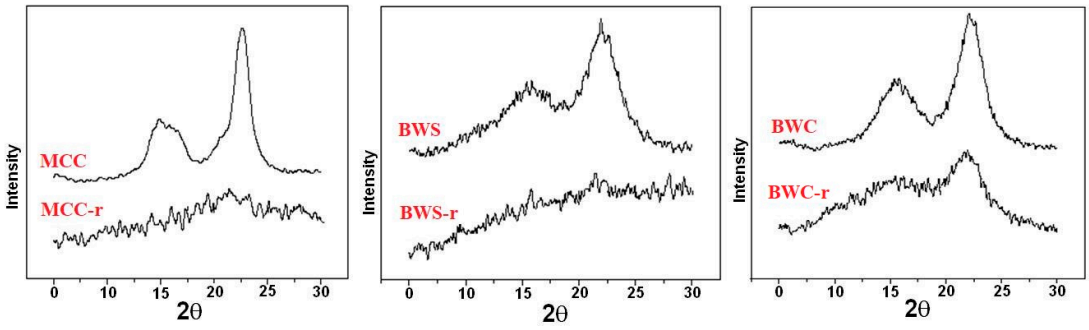


Figure 10. XRD diffractograms of microcrystalline cellulose (MCC), beech wood sawdust (BWS), respectively beech wood cellulose (BWC)—initial, and after regeneration process from ionic liquids MCC_r, BWS_r, and BWC_r. Permission to re-draw and reuse figures obtained from Romanian Academy, copyright holder [125].

The diffraction pattern of raw cellulose materials is characterized by a peak of high intensity around 23° (2θ) attributed to cellulose polymer. In comparison, the diffraction peaks of the regenerated material nearly disappeared from the XRD graph. However, some diffraction peaks, attributed probably to crystalline regions of cellulose, remained after regeneration and can be still observed at the same angle value. Moreover, the existence of non-crystalline structures in the material was confirmed by the appearance of the broad diffraction peaks in the range of 15 to 19° (2θ) [125].

An exemplification for estimation of CI values from XRD data (by means of the Segal method) for different cellulose substrates, initial and after various pre-treatments (with ionic liquid [BMIM]Cl; with ionic liquid and enzymatic hydrolysis using cellulase) is given in Table 3 as follows (data re-written from [31]).

Table 3. Estimation of CI values from XRD data (by means of Segal method) for different cellulose substrates, initial and after various pre-treatments.

Microcrystalline Cellulose	*Whatman Filter Paper*	*Industrial Softwood Cellulose Pulp*
0.7222 (initial)	0.7099 (initial)	0.3899 (initial)
0.7149 (enzyme)	0.4964 (enzyme)	0.5555 (enzyme)
0.2592 (ionic liquid IL)	0.3852 (ionic liquid IL)	0.1975 (ionic liquid IL)
0.4045 (IL and enzyme)	0.2523 (IL and enzyme)	0.4791 (IL and enzyme)

From these values, there can be observed differences between cellulose substrates in relation to their different degrees of crystallinity and susceptibility to further enzymatic treatment. The reduced crystalline part in cellulose substrates after treatment with IL has a positive effect when treatments are combined (IL with enzyme).

The XRD method was also efficiently applied to investigate the crystallinity of wood samples (mainly composed of cellulose), controlled and impregnated with natural products, vegetable oils, and natural wax (beeswax) [123], as presented in Figure 11. The diffractograms recorded for initial wood samples present the peaks, which are specific to the (002) crystal plane of cellulose from the wood structure near 2θ = 21θ, and to the amorphous region—a diffraction peak around 18θ). The peaks are more intense at the end of exposure to soil contact conditions. Overall, these patterns evidence a higher degree of crystallinity for wood impregnated with beeswax, but also to a lesser extent for the other wood samples under study, mostly after exposure to soil contact conditions. This evolution may be related to possible crystallization in the quasi-crystalline part of amorphous regions due to the rearrangement or reorientation of cellulose chains inside these regions under relatively high moisture conditions.

A rather novel approach is the development of ILs with low toxicity (such as [EMIM][OAc], choliniumlysinate ([Ch][Lys]), and ethanolamine acetate) that are able to assist the enzymatic saccharification of cellulose substrates without enzyme inactivation [224,225] and the design of new thermophilic enzyme mixtures able to act in the presence of typical ILs, such as [EMIM]OAc [226,227].

Furthermore, the deep eutectic solvents (DESs), a rather new group of green ionic solvents with low transition temperatures, may represent a viable alternative to ILs. An illustrative example is choline chloride/urea (ChCl/urea (1:2) that was able to solubilize up to 6% wt% Avicel PH-105 microcrystalline cellulose upon the anion exchange (Cl- exchange by OAc-) and addition of 15% tributyl methyl ammonium chloride [TBMA]Cl, which led to the formation of a new effective ionic solvent, namely [Ch]OAc/[TBMA]Cl [35]. The regenerated Avicel PH-105 cellulose was completely amorphous. DESs can be also obtained from renewable resources, such as ILs, using lignin and hemicelluloses derived aldehydes or phenols [228].

The main disadvantages of using ILs are connected to their high price and the requirement for their recovery and recycling. A rather new concept was developed, namely the use of low-cost ILs obtained from renewable resources. Thus, a series of tertiary amine-based ILs was synthesized from aromatic aldehydes derived from lignin and hemicellulose, the major by-products of lignocellulosic biofuel production [229,230]. The XRD study confirmed the IL treatment efficiency and showed the structural changes that subsequently

occurred in cellulose. The principles of the circular economy were thus applied in order to maximize the benefits of employing ILs in the conversion of cellulose substrates and to increase the potential of biomass refinery.

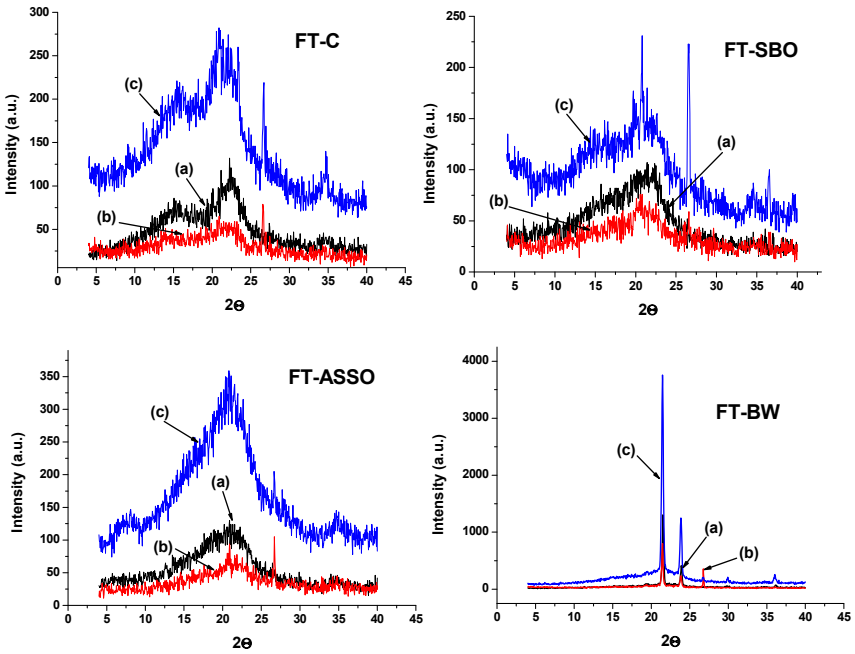


Figure 11. X-ray diffraction curves recorded for wood samples: (a) initial; (b) after 6 months degradation in soil; (c) after 12 months degradation in soil (where FT-C is initial fir tree wood samples as discs; FT-SBO fir tree wood impregnated with soybean oil; FT-ASSO is fir tree wood impregnated with *Asclepias syriaca* seed oil; FT-BW is fir tree wood impregnated with beeswax). Permission to re-draw and reuse figures obtained from C.-A. Teacă, copyright holder [123].

7. Conclusions

The crystallinity of cellulosic substrates is a key factor in their processability, as well as an indication of their susceptibility to undergo sensitive reactions (such as enzymatic saccharification) with high yields. Since high crystalline substrates resist hydrolytic attack, it was necessary to reduce their crystallinity by various methods: physical–grinding and hydrothermal treatments; chemical–alkaline, acidic, and redox hydrolysis; solvolysis–ILs; radiative–plasma and high energy irradiation; and biological–enzyme hydrolysis. All of them provided cellulosic substrates with increased purity, reduced particle size, and, most of all, reduced crystallinity and, hence, enhanced availability of cellulose for hydrolysis.

FT-IR and X-ray diffraction spectroscopy are useful, reliable, and easy-to-reach solid-state characterization methods for assessing the crystallinity of different cellulose substrates. Due to their specific methodology, they can be used to analyze not only starting materials and their final products but also intermediates. This allowed users to monitor processes in their entirety, follow dynamic changes in the structure of substrates, identify reactive metastable species, and the formation of new chemical and/or physical bonds. Data obtained by these methods substantiated the structural changes in cellulosic substrates, as well as the alterations that occurred in their supramolecular architectures.

Useful insights have been achieved by employing these methods to evaluate crystallinity changes determined by structural modification of different cellulose substrates. For example, FT-IR confirmed the cellulose I polymorph form in the structure of all initial substrates, the disruption of hydrogen bonds during solubilization in ILs, and the formation of allomorph cellulose II by regeneration, which has a lower crystallinity than cellulose I due to its antiparallel chain orientation. Even more, XRD substantiated that, under spe-

cific conditions (alkaline treatment in the presence of liquid ammonia), cellulose I and II may undergo a further crystalline transition to polymorphs cellulose III_I and III_{II} along with a significant decrease in crystallinity. At the same time, the conversion of crystalline cellulose I into amorphous cellulose II during enzymatic saccharification, with or without pre-treatment (solubilization in ILs), was evidenced beyond any reasonable doubt by FT-IR and XRD experimental results, which thus confirmed the corresponding theories.

In recent years, other analysis methods have been investigated that can be used to evaluate the crystallinity of cellulosic substrates, such as FT Raman spectroscopy, solid-state ^{13}C NMR, quantitative ^{13}C MultiCP solid-state NMR, or even physicochemical methods, based on the measurements of sorption of water vapor and the enthalpy of wetting. Despite the advantages of these new methods, FT-IR and X-ray diffraction spectroscopy remain the first choice as they provide fast and reliable results, can be used in both qualitative and quantitative studies, and involve simple and straightforward procedures. Some developments of these methods have already been proposed (i.e., an X-ray diffraction method where Rietveld refinement was applied with consideration of the March–Dollase preferred orientation at the (001) plane), but all improvements in terms of accuracy and reliability are welcome.

Author Contributions: Conceptualization, M.-C.S., F.T. and C.-A.T.; methodology, M.-C.S., F.T. and C.-A.T.; software, M.-C.S.; validation, M.-C.S., F.T. and C.-A.T.; formal analysis, C.-A.T.; investigation, M.-C.S., F.T. and C.-A.T.; resources, C.-A.T.; data curation, C.-A.T.; writing—original draft preparation, M.-C.S., F.T. and C.-A.T.; writing—review and editing, M.-C.S., F.T. and C.-A.T.; visualization, C.-A.T.; supervision, C.-A.T. All authors have read and agreed to the published version of the manuscript.

Funding: This research received no external funding.

Institutional Review Board Statement: Not applicable.

Data Availability Statement: No new data were created or analyzed in this study.

Acknowledgments: We dedicate this paper to the memory of our dear colleague and friend, Ruxanda Bodîrlău, who passed away on 26 June 2016, and honor her demure support and enthusiastic work. The authors also acknowledge the significant contribution of Eng. Elena Marlică, as concerns the XRD studies.

Conflicts of Interest: The authors declare no conflicts of interest.

References

1. Klemm, D.; Heublein, B.; Fink, H.P.; Bohn, A. Cellulose: Fascinating biopolymer and sustainable raw material. *Angew. Chem. Int. Ed.* **2005**, *44*, 3358–3393. [CrossRef] [PubMed]
2. Ragauskas, A.J.; Williams, C.K.; Davison, B.H.; Britovsek, G.; Cairney, J.; Eckert, C.A.; Frederick, W.J., Jr.; Hallett, J.P.; Leak, D.J.; Liotta, C.L.; et al. The path forward for biofuels and biomaterials. *Science* **2006**, *311*, 484–489. [CrossRef] [PubMed]
3. Ragauskas, A.J.; Beckham, G.T.; Biddy, M.J.; Chandra, R.; Chen, F.; Davis, M.F.; Davison, B.H.; Dixon, R.A.; Gilna, P.; Keller, M.; et al. Lignin valorization: Improving lignin processing in the biorefinery. *Science* **2014**, *344*, 124684. [CrossRef] [PubMed]
4. Laurichesse, S.; Avérous, L. Chemical modification of lignins: Towards biobased polymers. *Prog. Polym. Sci.* **2014**, *39*, 1266–1290. [CrossRef]
5. Collins, M.N.; Nechifor, M.; Tanasă, F.; Zănoagă, M.; McLoughlin, A.; Stróżyk, M.A.; Culebras, M.; Teacă, C.-A. Valorization of lignin in polymer and composite systems for advanced engineering applications—A review. *Int. J. Biol. Macromol.* **2019**, *131*, 828–849. [CrossRef]
6. Gröndahl, J.; Karisalmim, K.; Vapaavuori, J. Micro-and nanocelluloses from non-wood waste sources; processes and use in industrial applications. *Soft Matter* **2021**, *17*, 9842–9858. [CrossRef]
7. Magalhães, S.; Fernandes, C.; Pedrosa, J.F.S.; Alves, L.; Medronho, B.; Ferreira, P.J.T.; Rasteiro, M.d.G. Eco-Friendly Methods for Extraction and Modification of Cellulose: An Overview. *Polymers* **2023**, *15*, 3138. [CrossRef]
8. Martinelli, A.; Giannini, L.; Branduardi, P. Enzymatic Modification of Cellulose to Unlock Its Exploitation in Advanced Materials. *ChemBioChem A Eur. J. Chem. Biol.* **2021**, *22*, 974–981. [CrossRef]

9. Machado, B.; Costa, S.M.; Costa, I.; Fangueiro, R.; Ferreira, D.P. The potential of algae as a source of cellulose and its derivatives for biomedical applications. *Cellulose* **2024**, *31*, 3353–3376. [CrossRef]
10. Rol, F.; Belgacem, M.N.; Gandini, A.; Bras, J. Recent advances in surface-modified cellulose nanofibrils. *Prog. Polym. Sci.* **2019**, *88*, 241–264. [CrossRef]
11. Rajinipriya, M.; Nagalakshmaiah, M.; Robert, M.; Elkoun, S. Importance of Agricultural and Industrial Waste in the Field of Nanocellulose and Recent Industrial Developments of Wood Based Nanocellulose: A Review. *ACS Sustainable Chem. Eng.* **2018**, *6*, 2807–2828. [CrossRef]
12. Kulasinski, K.; Keten, S.; Churakov, S.; Derome, D.; Carmeliet, J. A comparative molecular dynamics study of crystalline, paracrystalline and amorphous states of cellulose. *Cellulose* **2014**, *21*, 1103–1116. [CrossRef]
13. Ioelovich, M.; Leykin, A.; Figovsky, O. Study of cellulose paracrystallinity. *BioResources* **2010**, *5*, 1393–1407. [CrossRef]
14. Wang, C.; Su, J.; Liu, T.; Ge, S.; Liew, R.K.; Zhang, H.; Naushad, M.; Lam, S.S.; Ng, H.S.; Sonne, C.; et al. A sustainable strategy to transform cotton waste into renewable cellulose fiber self-reinforcing composite paper. *J. Clean. Prod.* **2023**, *429*, 139567. [CrossRef]
15. Wei, D.W.; Wei, H.; Gauthier, A.C.; Song, J.; Jin, Y.; Xiao, H. Superhydrophobic modification of cellulose and cotton textiles: Methodologies and applications. *J. Biores. Bioprod.* **2020**, *5*, 1–15. [CrossRef]
16. Lee, K.-Y.; Buldum, G.; Mantalaris, A.; Bismarck, A. More Than Meets the Eye in Bacterial Cellulose: Biosynthesis, Bioprocessing, and Applications in Advanced Fiber Composites. *Macromol. Biosci.* **2014**, *14*, 10–32. [CrossRef]
17. Taokaew, S.; Kriangkrai, W. Recent Progress in Processing Cellulose Using Ionic Liquids as Solvents. *Polysaccharides* **2022**, *3*, 671–691. [CrossRef]
18. Fan, L.T.; Lee, Y.-H. Mechanism of the enzymatic hydrolysis of cellulose: Effects of major structural features of cellulose on enzymatic hydrolysis. *Biotechnol. Bioeng.* **1980**, *22*, 177–199. [CrossRef]
19. Isikgor, F.H.; Becer, C.R. Lignocellulosic biomass: A sustainable platform for the production of bio-based chemicals and polymers. *Polym. Chem.* **2015**, *6*, 4497–4559. [CrossRef]
20. Zhou, C.-H.; Xia, X.; Lin, C.-X.; Tong, D.-S.; Beltramini, J. Catalytic conversion of lignocellulosic biomass to fine chemicals and fuels. *Chem. Soc. Rev.* **2011**, *40*, 5588–5611. [CrossRef]
21. Cherubini, F.; Strømman, A.H. Chemicals from lignocellulosic biomass: Opportunities, perspectives, and potential of biorefinery systems. *Biofuels Bioprod. Biorefin.* **2011**, *5*, 548–561. [CrossRef]
22. Corma, A.; Iborra, S.; Velty, A. Chemical routes for the transformation of biomass into chemicals. *Chem. Rev.* **2007**, *107*, 2411–2502. [CrossRef] [PubMed]
23. Gallezot, P. Process options for converting renewable feedstocks to bioproducts. *Green Chem.* **2007**, *9*, 295–302. [CrossRef]
24. Huber, G.W.; Iborra, S.; Corma, A. Synthesis of transportation fuels from biomass: Chemistry, catalysts, and engineering. *Chem. Rev.* **2006**, *106*, 4044–4098. [CrossRef]
25. Bhatia, S.K.; Jagtap, S.S.; Bedekar, A.A.; Bhatia, R.K.; Patel, A.K.; Pant, D.; Rajesh Banu, J.; Rao, C.V.; Kim, Y.G.; Yang, Y.H. Recent developments in pretreatment technologies on lignocellulosic biomass: Effect of Key parameters, technological improvements, and challenges. *Bioresour. Technol.* **2020**, *300*, 122724. [CrossRef]
26. Kaur, D.; Bhardwaj, N.K.; Lohchab, R.K. Impact of modifying conventional chlorine dioxide stage to hot chlorine dioxide during rice straw pulp bleaching on pulp, paper and effluent characteristics. *Cellulose* **2019**, *26*, 7469–7482. [CrossRef]
27. Anderson, E.M.; Stone, M.L.; Katahira, R.; Reed, M.; Beckham Gr, T.; Roman-Leshkov, Y. Flowthrough reductive catalytic fractionation of biomass. *Joule* **2017**, *1*, 613–622. [CrossRef]
28. Singh, S.K. Biological treatment of plant biomass and factors affecting bioactivity. *J. Clean. Prod.* **2021**, *279*, 123546. [CrossRef]
29. Seidl, P.R.; Goulart, A.K. Pretreatment processes for lignocellulosic biomass conversion to biofuels and bioproducts. *Curr. Opin. Green Sustain. Chem.* **2016**, *2*, 48–53. [CrossRef]
30. Nguyen, T.Y.; Cai, C.M.; Kumar, R.; Wyman, C.E. Co-solvent pretreatment reduces costly enzyme requirements for high sugar and ethanol yields from lignocellulosic biomass. *ChemSusChem* **2015**, *8*, 1716–1725. [CrossRef]
31. Teacă, C.-A.; Stanciu, M.-C.; Tanasă, F.; Nechifor, M. Ionic liquids for enhanced enzymatic saccharification of cellulose based materials. In *Nanotechnology Based Industrial Applications of Ionic Liquids, Inamuddin*; Asiri, A., Ed.; Springer Nature Switzerland AG: Cham, Switzerland, 2020. [CrossRef]
32. Liao, Y.; de Beeck, B.O.; Thielemans, K.; Ennaert, T.; Snelders, J.; Dusselier, M.; Courtin, C.M.; Sels, B.F. The role of pretreatment in the catalytic valorization of cellulose. *Mol. Catal.* **2020**, *487*, 110883. [CrossRef]
33. Singh, S.; Cheng, G.; Sathitsuksanoh, N.; Wu, D.; Varanasi, P.; George, A.; Balan, V.; Gao, X.; Kumar, R.; Dale, B.E.; et al. Comparison of different biomass pretreatment techniques and their impact on chemistry and structure. *Front. Energy Res.* **2015**, *2*, 62. [CrossRef]
34. Zhang, Q.; Jérôme, F. Mechanocatalytic deconstruction of cellulose: An emerging entry into biorefinery. *ChemSusChem* **2013**, *6*, 2042–2044. [CrossRef] [PubMed]
35. Zhang, Q.; Benoit, M.; De Oliveira Vigier, K.; Barrault, J.; Jérôme, F. Green and inexpensive choline-derived solvents for cellulose decrystallization. *Chem. Eur. J.* **2012**, *18*, 1043–1046. [CrossRef]

36. Wang, Y.; Lindström, M.E.; Henriksson, G. Increased degradability of cellulose by dissolution in cold alkali. *BioResources* **2014**, *9*, 7566–7578. [CrossRef]
37. Atalla, R.H.; Vanderhart, D.L. Native cellulose: A composite of two distinct crystalline forms. *Science* **1984**, *223*, 283–285. [CrossRef]
38. Sugiyama, J.; Vuong, R.; Chanzy, H. Electron diffraction study on the two crystalline phases occurring in native cellulose from an algal cell wall. *Macromolecules* **1991**, *24*, 4168–4175. [CrossRef]
39. Viëtor, R.J.; Newman, R.H.; Ha, M.A.; Apperley, D.C.; Jarvis, M.C. Conformational features of crystal-surface cellulose from higher plants. *Plant J.* **2002**, *30*, 721–731. [CrossRef]
40. Zugenmaier, P. Conformation and packing of various crystalline cellulose fibers. *Prog. Polym. Sci.* **2001**, *26*, 1341–1417. [CrossRef]
41. O'Sullivan, A.C. Cellulose: The structure slowly unravels. *Cellulose* **1997**, *4*, 173–207. [CrossRef]
42. Wohlert, M.; Benselfelt, T.; Wågberg, L.; Furó, I.; Berglund, L.A.; Wohlert, J. Cellulose and the role of hydrogen bonds: Not in charge of everything. *Cellulose* **2022**, *29*, 1–23. [CrossRef]
43. Zhao, H.; Kwak, J.H.; Wang, Y.; Franz, J.A.; White, J.M.; Holladay, J.E. Effects of crystallinity on dilute acid hydrolysis of cellulose by cellulose ball-milling study. *Energy Fuels* **2006**, *20*, 807–811. [CrossRef]
44. He, Y.-C.; Liu, F.; Gong, L.; Zhu, Z.-Z.; Ding, Y.; Wang, C.; Xue, Y.-F.; Rui, H.; Tao, Z.-C.; Zhang, D.-P.; et al. Significantly improving enzymatic saccharification of high crystallinity index's corn stover by combining ionic liquid [Bmim]Cl–HCl–water media with dilute NaOH pretreatment. *Bioresour. Technol.* **2015**, *189*, 421–425. [CrossRef] [PubMed]
45. Cui, T.; Li, J.; Yan, Z.; Yu, M.; Li, S. The correlation between the enzymatic saccharification and the multidimensional structure of cellulose changed by different pretreatments. *Biotechnol. Biofuels* **2014**, *7*, 134. [CrossRef]
46. Samayam, I.P.; Hanson, B.L.; Langan, P.; Schall, C.A. Ionic-liquid induced changes in cellulose structure associated with enhanced biomass hydrolysis. *Biomacromolecules* **2011**, *12*, 3091–3098. [CrossRef]
47. Cho, H.M.; Gross, A.S.; Chu, J. Dissecting force interactions in cellulose deconstruction reveals the required solvent versatility for overcoming biomass recalcitrance. *J. Am. Chem. Soc.* **2011**, *133*, 14033–14041. [CrossRef]
48. Zhang, Y.-H.P.; Lynd, L.R. Toward an aggregated understanding of enzymatic hydrolysis of cellulose: Noncomplexed cellulose systems. *Biotechnol. Bioeng.* **2004**, *88*, 797–824. [CrossRef]
49. Zhang, Y.H.P. Reviving the carbohydrate economy via multi-product biorefineries. *J. Ind. Microbiol. Biotechnol.* **2008**, *35*, 367–375. [CrossRef]
50. Zhang, Y.H.P.; Hong, J.; Ye, X. Cellulase assays. In *Biofuels: Methods and Protocols, Methods in Molecular Biology*; Mielenz, J.R., Ed.; Humana Press (A Part of Springer Science + Business Media, LLC.): Totowa, NJ, USA, 2009; Volume 581. [CrossRef]
51. Zhang, Y.-H.P.; Himmel, M.; Mielenz, J.R. Outlook for cellulase improvement: Screening and selection strategies. *Biotechnol. Adv.* **2006**, *24*, 452–481. [CrossRef]
52. Hall, M.; Bansal, P.; Lee, J.H.; Realff, M.J.; Bommarius, A.S. Cellulose crystallinity—A key predictor of the enzymatic hydrolysis rate. *FEBS J.* **2010**, *277*, 1571–1582. [CrossRef]
53. Tadesse, H.; Luque, R. Advances on biomass pretreatment using ionic liquids: An overview. *Energy Environ. Sci.* **2011**, *4*, 3913–3929. [CrossRef]
54. Bodîrlău, R.; Teacă, C.-A.; Spiridon, I. Influence of ionic liquid on hydrolyzed cellulose material: FT-IR spectroscopy and TG-DTG-DSC analysis. *Int. J. Polym. Anal. Charact.* **2010**, *15*, 460–469. [CrossRef]
55. Bodîrlău, R.; Teacă, C.-A.; Spiridon, I. Enzymatic hydrolysis of Asclepias syriaca fibers in the presence of ionic liquids. *Monatsh. Chem.* **2010**, *141*, 1043–1048. [CrossRef]
56. Spiridon, I.; Teacă, C.-A.; Bodîrlău, R. Structural changes evidenced by FTIR spectroscopy in cellulosic materials after pre-treatment with ionic liquid and enzymatic hydrolysis. *BioResources* **2011**, *6*, 400–413. [CrossRef]
57. Geng, X.; Henderson, W.A. Impact of non-solvents on the structural features and enzymatic digestibility of cellulose regenerated from an ionic liquid. *RSC Adv.* **2014**, *4*, 31226–31229. [CrossRef]
58. Shamshina, J.L.; Abidi, N. Cellulose nanocrystals from ionic liquids: A critical review. *Green Chem.* **2021**, *23*, 6205–6222. [CrossRef]
59. Kosan, B.; Michels, C.; Meister, F. Dissolution and forming of cellulose with ionic liquids. *Cellulose* **2008**, *15*, 59–66. [CrossRef]
60. van Rantwijk, F.; Sheldon, R.A. Biocatalysis in ionic liquids. *Chem. Rev.* **2007**, *107*, 2757–2785. [CrossRef]
61. Dadi, A.P.; Varanasi, S.; Schall, C.A. Enhancement of cellulose saccharification kinetics using an ionic liquid pretreatment step. *Biotechnol. Bioeng.* **2006**, *95*, 904–910. [CrossRef]
62. Kamiya, N.; Matsushita, Y.; Hanaki, M.; Nakashima, K.; Narita, M.; Goto, M.; Takahashi, H. Enzymatic in situ saccharification of cellulose in aqueous-ionic liquid media. *Biotechnol. Lett.* **2008**, *30*, 1037–1040. [CrossRef]
63. Zhao, H.; Baker, G.A.; Cowins, J.V. Fast enzymatic saccharification of switchgrass after pretreatment with ionic liquids. *Biotechnol. Prog.* **2010**, *26*, 127–133. [CrossRef] [PubMed]
64. Xu, J.; Liu, X.; He, J.; Hu, L.; Dai, B.; Wu, B. Enzymatic in situ saccharification of rice straw in aqueous-ionic liquid media using encapsulated Trichoderma aureoviride cellulose. *J. Chem. Technol. Biotechnol.* **2015**, *90*, 57–63. [CrossRef]

65. Kassanov, B.; Wang, J.; Fu, Y.; Chang, J. Cellulose enzymatic saccharification and preparation of 5-hydroxymethylfurfural based on bamboo hydrolysis residue separation in ionic liquids. *RSC Adv.* **2017**, *7*, 30755–30762. [CrossRef]
66. Ishida, T. Theoretical Investigation of Dissolution and Decomposition Mechanisms of a Cellulose Fiber in Ionic Liquids. *J. Phys. Chem. B* **2020**, *124*, 3090–3102. [CrossRef]
67. El Seoud, O.A.; Kostag, M.; Jedvert, K.; Malek, N.I. Cellulose in Ionic Liquids and Alkaline Solutions: Advances in the Mechanisms of Biopolymer Dissolution and Regeneration. *Polymers* **2019**, *11*, 1917. [CrossRef]
68. Ling, Z.; Chen, S.; Zhang, X.; Takabe, K.; Xu, F. Unraveling variations of crystalline cellulose induced by ionic liquid and their effects on enzymatic hydrolysis. *Sci. Rep.* **2017**, *7*, 10230. [CrossRef]
69. Li, C.; Cheng, G.; Balan, V.; Kent, M.S.; Ong, M.; Chundawat, S.; daCosta Sousa, P.S.; Melnichenko, Y.B.; Dale, B.E.; Simmons, B.A.; et al. Influence of physico-chemical changes on enzymatic digestibility of ionic liquid and AFEX pretreated corn stover. *Bioresour. Technol.* **2011**, *102*, 6928–6936. [CrossRef]
70. Jin, L.; Yu, X.; Peng, C.; Guo, Y.; Zhang, L.; Xu, Q.; Zhao, Z.K.; Liu, Y.; Xie, H. Fast dissolution pretreatment of the corn stover in gamma-valerolactone promoted by ionic liquids: Selective delignification and enhanced enzymatic saccharification. *Bioresour. Technol.* **2018**, *270*, 537–544. [CrossRef]
71. Cheenkachorn, K.; Douzou, T.; Roddecha, S.; Tantayotai, P.; Sriariyanun, M. Enzymatic saccharification of rice straw under influence of recycled ionic liquid pretreatments. *Energy Procedia* **2016**, *100*, 160–165. [CrossRef]
72. Ren, H.; Zong, M.-H.; Wu, H.; Li, N. Efficient pretreatment of wheat straw using novel renewable cholinium ionic liquids to improve enzymatic saccharification. *Ind. Eng. Chem. Res.* **2016**, *55*, 1788–1795. [CrossRef]
73. Ninomiya, K.; Kamide, K.; Takahashi, K.; Shimizu, N. Enhanced enzymatic saccharification of kenaf powder after ultrasonic pretreatment in ionic liquids at room temperature. *Bioresour. Technol.* **2012**, *103*, 259–265. [CrossRef] [PubMed]
74. Singh, S.; Simmons, B.A.; Vogel, K.P. Visualization of biomass solubilization and cellulose regeneration during ionic liquid pretreatment of switchgrass. *Biotechnol. Bioeng.* **2009**, *104*, 68–75. [CrossRef] [PubMed]
75. Li, C.; Knierim, B.; Manisseri, C.; Arora, R.; Scheller, H.V.; Auer, M.; Vogel, K.P.; Simmons, B.A.; Singh, S. Comparison of dilute acid and ionic liquid pretreatment of switchgrass: Biomass recalcitrance, delignification and enzymatic saccharification. *Bioresour. Technol.* **2010**, *101*, 4900–4906. [CrossRef] [PubMed]
76. Samayam, I.P.; Schall, C.A. Saccharification of ionic liquid pretreated biomass with commercial enzyme mixtures. *Bioresour. Technol.* **2010**, *101*, 3561–3566. [CrossRef]
77. Uju, N.A.; Shoda, Y.; Goto, M.; Tokuhara, W.; Noritake, Y.; Katahira, S.; Ishida, N.; Ogino, C.; Kamiya, N. Low melting point pyridinium ionic liquid pretreatment for enhancing enzymatic saccharification of cellulosic biomass. *Bioresour. Technol.* **2013**, *135*, 103–108. [CrossRef]
78. Uju, N.A.; Shoda, Y.; Nakamoto, A.; Goto, M.; Tokuhara, W.; Noritake, Y.; Katahira, S.; Ishida, N.; Nakashima, K.; Ogino, C.; et al. Short time ionic liquids pretreatment on lignocellulosic biomass to enhance enzymatic saccharification. *Bioresour. Technol.* **2012**, *103*, 446–452. [CrossRef]
79. Wang, Y.; Radosevich, M.; Hayes, D.; Labbé, N. Compatible ionic liquid-cellulases system for hydrolysis of lignocellulosic biomass. *Biotechnol. Bioeng.* **2011**, *108*, 1042–1048. [CrossRef]
80. Xu, J.; Liu, B.; Hou, H.; Hu, J. Pretreatment of eucalyptus with recycled ionic liquids for low-cost biorefinery. *Bioresour. Technol.* **2017**, *234*, 406–414. [CrossRef]
81. Li, H.Y.; Chen, X.; Wang, C.Z.; Sun, S.N.; Sun, R.C. Evaluation of the two-step treatment with ionic liquids and alkali for enhancing enzymatic hydrolysis of Eucalyptus: Chemical and anatomical changes. *Biotechnol. Biofuels* **2016**, *9*, 166. [CrossRef]
82. Dadi, A.P.; Schall, C.A.; Varanasi, S. Mitigation of cellulose recalcitrance to enzymatic hydrolysis by ionic liquid pretreatment. *Appl. Biochem. Biotechnol.* **2007**, *137*, 407–421. [CrossRef]
83. Cheng, G.; Varanasi, P.; Li, C.; Liu, H.; Melnichenko, Y.B.; Simmons, B.A.; Kent, M.S.; Singh, S. Transition of cellulose crystalline structure and surface morphology of biomass as a function of ionic liquid pretreatment and its relation to enzymatic hydrolysis. *Biomacromolecules* **2011**, *12*, 933–941. [CrossRef] [PubMed]
84. Bian, J.; Peng, F.; Peng, X.; Xiao, X.; Peng, P.; Xu, F.; Sun, R. Effect of [Emim]Ac pretreatment on the structure and enzymatic hydrolysis of sugarcane bagasse cellulose. *Carbohydr. Polym.* **2014**, *100*, 211–217. [CrossRef] [PubMed]
85. Uto, T.; Yamamoto, K.; Kadokawa, J. Cellulose Crystal Dissolution in Imidazolium-Based Ionic Liquids: A Theoretical Study. *J. Phys. Chem. B* **2017**, *122*, 258–266. [CrossRef] [PubMed]
86. Endo, T.; Fujii, S.; Aung, E.M.; Kuroda, K.; Tsukegi, T.; Ninomiya, K.; Takahashi, K. Cellulose structural change in various biomass species pretreated by ionic liquid at different biomass loadings. *BioResources* **2019**, *13*, 6663–6677.
87. Hou, X.; Li, N.; Zong, M. Renewable bio ionic liquids-water mixtures-mediated selective removal of lignin from rice straw: Visualization of changes in composition and cell wall structure. *Biotechnol. Bioeng.* **2013**, *110*, 1895–1902. [CrossRef]
88. Hou, X.; Li, N.; Zong, M. Significantly enhancing enzymatic hydrolysis of rice straw after pretreatment using renewable ionic liquid–water mixtures. *Bioresour. Technol.* **2013**, *136*, 469–474. [CrossRef]

89. Hou, X.; Smith, T.J.; Li, N.; Zong, M. Novel renewable ionic liquids as highly effective solvents for pretreatment of rice straw biomass by selective removal of lignin. *Biotechnol. Bioeng.* **2012**, *109*, 2484–2493. [CrossRef]
90. Brandt, A.; Gräsvik, J.; Hallett, J.P.; Welton, T. Deconstruction of lignocellulosic biomass with ionic liquids. *Green Chem.* **2013**, *15*, 550–583. [CrossRef]
91. Sun, N.; Jiang, X.; Maxim, M.L.; Metlen, A.; Rogers, R.D. Use of polyoxometalate catalysts in ionic liquids to enhance the dissolution and delignification of woody biomass. *ChemSusChem* **2011**, *4*, 65–73. [CrossRef]
92. Miyafuji, H. Application of ionic liquids for effective use of woody biomass. *J. Wood Sci.* **2015**, *61*, 343–350. [CrossRef]
93. Fort, D.A.; Remsing, R.C.; Swatloski, R.P.; Moyna, P.; Moyna, G.; Rogers, R.D. Can ionic liquids dissolve wood? Processing and analysis of lignocellulosic materials with 1-N-butyl-3-methylimidazolium chloride. *Green Chem.* **2007**, *9*, 63–69. [CrossRef]
94. Kilpeläinen, I.; Xie, H.; King, A.; Granstrom, M.; Heikkinen, S.; Argyropoulos, D.S. Dissolution of wood in ionic liquids. *J. Agric. Food Chem.* **2007**, *55*, 9142–9148. [CrossRef] [PubMed]
95. Gericke, M.; Fardim, P.; Heinze, T. Ionic liquids—Promising but challenging solvents for homogeneous derivatization of cellulose. *Molecules* **2012**, *17*, 7458–7502. [CrossRef] [PubMed]
96. Pang, Z.; Dong, C.; Pan, X. Enhanced deconstruction and dissolution of lignocellulosic biomass in ionic liquid at high water content by lithium chloride. *Cellulose* **2015**, *23*, 323–338. [CrossRef]
97. Mansfield, S.D.; Mooney, C.; Saddler, J.N. Substrate and enzyme characteristics that limit cellulose hydrolysis. *Biotechnol. Prog.* **1999**, *15*, 804–816. [CrossRef]
98. Kumar, R.; Wyman, C.E. Physical and chemical features of pretreated biomass that influence macro-/micro-accessibility and biological processing. In *Aqueous Pretreatment of Plant Biomass for Biological and Chemical Conversion to Fuels and Chemicals*; Wyman, C.E., Ed.; John Wiley and Sons Ltd.: West Sussex, UK, 2013; pp. 281–310. [CrossRef]
99. Segal, L.; Creely, J.J.; Martin, A.E., Jr.; Conrad, C.M. An empirical method for estimating the degree of crystallinity of native cellulose using the X-ray diffractometer. *Text. Res. J.* **1959**, *29*, 786–794. [CrossRef]
100. Åkerholm, M.; Hinterstoisser, B.; Salmén, L. Characterization of the crystalline structure of cellulose using static and dynamic FT-IR spectroscopy. *Carbohydr. Res.* **2004**, *339*, 569–578. [CrossRef]
101. Leppänen, K.; Andersson, S.; Torkkeli, M.; Knaapila, M.; Kotelnikova, N.; Serimaa, R. Structure of cellulose and microcrystalline cellulose from various wood species, cotton and flax studied by X-ray scattering. *Cellulose* **2009**, *16*, 999–1015. [CrossRef]
102. Park, S.; Baker, J.O.; Himmel, M.E.; Parilla, P.A.; Johnson, D.K. Cellulose crystallinity index: Measurement techniques and their impact on interpreting cellulase performance. *Biotechnol. Biofuels* **2010**, *3*, 10. [CrossRef]
103. Park, S.; Johnson, D.K.; Ishizawa, C.I.; Parilla, P.A.; Davis, M.F. Measuring the crystallinity index of cellulose by solid state 13C nuclear magnetic resonance. *Cellulose* **2009**, *16*, 641–647. [CrossRef]
104. Agarwal, U.P.; Reiner, R.S.; Ralph, S.A. Cellulose I crystallinity determination using FT-Raman spectroscopy: Univariate and multivariate methods. *Cellulose* **2010**, *17*, 721–733. [CrossRef]
105. French, A.D.; Santiago Cintrón, M. Cellulose polymorphy, crystallite size, and the Segal Crystallinity Index. *Cellulose* **2013**, *20*, 583–588. [CrossRef]
106. Barnette, A.L.; Bradley, L.C.; Veres, B.D.; Schreiner, E.P.; Park, Y.B.; Park, J.; Park, S.; Kim, S.H. Selective detection of crystalline cellulose in plant cell walls with sum-frequency-generation (SFG) vibration spectroscopy. *Biomacromolecules* **2011**, *12*, 2434–2439. [CrossRef] [PubMed]
107. Barnette, A.L.; Lee, C.; Bradley, L.C.; Schreiner, E.P.; Park, Y.B.; Shin, H.; Cosgrove, D.J.; Park, S.; Kim, S.H. Quantification of crystalline cellulose in lignocellulosic biomass using sum frequency generation (SFG) vibration spectroscopy and comparison with other analytical methods. *Carbohydr. Polym.* **2012**, *89*, 802–809. [CrossRef]
108. Makarem, M.; Lee, C.M.; Kafle, K.; Huang, S.; Chae, I.; Yang, H.; Kubicki, J.D.; Kim, S.H. Probing cellulose structures with vibrational cellulose structures with vibrational spectroscopy. *Cellulose* **2019**, *26*, 35–79. [CrossRef]
109. Salem, K.S.; Kasera, N.K.; Rahman, M.A.; Jameel, H.; Habibi, Y.; Eichhorn, S.J.; French, A.D.; Pal, L.; Lucia, L.A. Comparison and assessment of methods for cellulose crystallinity determination. *Chem. Soc. Rev.* **2023**, *52*, 6417–6446. [CrossRef]
110. Montoya-Escobar, N.; Ospina-Acero, D.; Velásquez-Cock, J.A.; Gómez-Hoyos, C.; Serpa Guerra, A.; Gañan Rojo, P.F.; Vélez Acosta, L.M.; Escobar, J.P.; Correa-Hincapié, N.; Triana-Chávez, O.; et al. Use of Fourier Series in X-ray Diffraction (XRD) Analysis and Fourier-Transform Infrared Spectroscopy (FTIR) for Estimation of Crystallinity in Cellulose from Different Sources. *Polymers* **2022**, *14*, 5199. [CrossRef]
111. Agarwal, U.P.; Ralph, S.A.; Baez, C.; Reiner, R.S.; Verrill, S.P. Effect of sample moisture content on XRD-estimated cellulose crystallinity index and crystallite size. *Cellulose* **2017**, *24*, 1971–1984. [CrossRef]
112. Evans, R.; Newman, R.H.; Roick, U.C.; Suckling, I.D.; Wallis, A.F.A. Changes in cellulose crystallinity during kraft pulping. Comparison of infrared, X-ray diffraction and solid state NMR results. *Wood Res. Technol. Holzforschung* **1995**, *49*, 498–504. [CrossRef]
113. Kataoka, Y.; Kondo, T. FT-IR microscopic analysis of changing cellulose crystalline structure during wood cell wall formation. *Macromolecules* **1998**, *31*, 760–764. [CrossRef]

114. O'Connor, R.T.; DuPré, E.F.; Mitcham, D. Applications of infrared absorption spectroscopy to investigations of cotton and modified cottons. Part I: Physical and crystalline modifications and oxidation. *Text. Res. J.* **1958**, *28*, 382–392. [CrossRef]
115. Hurtubise, F.G.; Krassig, H. Classification of fine structural characteristics in cellulose by infrared spectroscopy. Use of potassium bromide pellet technique. *Anal. Chem.* **1960**, *32*, 177–181. [CrossRef]
116. Oh, S.Y.; Dong, I.Y.; Shin, Y.; Hwan, C.K.; Hak, Y.K.; Yong, S.C.; Won, H.P.; Ji, H.Y. Crystalline structure analysis of cellulose treated with sodium hydroxide and carbon dioxide by means of X-ray diffraction and FTIR spectroscopy. *Carbohydr. Res.* **2005**, *340*, 2376–2391. [CrossRef] [PubMed]
117. Nelson, M.L.; O'Connor, R.T. Relation of certain infrared bands to cellulose crystallinity and crystal lattice type. Part II. A new infrared ratio for estimation of crystallinity in celluloses I and II. *J. Appl. Polym. Sci.* **1964**, *8*, 1325–1341. [CrossRef]
118. Nada, A.-A.M.A.; Kamel, S.; El-Sakhawy, M. Thermal behaviour and infrared spectroscopy of cellulose carbamates. *Polym. Degrad. Stab.* **2000**, *70*, 347–355. [CrossRef]
119. Ling, Z.; Chen, S.; Zhang, X.; Xu, F. Exploring crystalline-structural variations of cellulose during alkaline pretreatment for enhanced enzymatic hydrolysis. *Biores. Technol.* **2017**, *224*, 611–617. [CrossRef]
120. Driemeier, C.; Calligaris, G.A. Theoretical and experimental developments for accurate determination of crystallinity of cellulose I materials. *J. Appl. Cryst.* **2011**, *44*, 184–192. [CrossRef]
121. Thygesen, A.; Oddershede, J.; Lilholt, H.; Thomsen, A.B.; Ståhl, K. On the determination of crystallinity and cellulose content in plant fibres. *Cellulose* **2005**, *12*, 563–576. [CrossRef]
122. Bansal, P.; Hall, M.; Realff, M.J.; Lee, J.H.; Bommarius, A.S. Multivariate statistical analysis of X-ray data from cellulose: A new method to determine degree of crystallinity and predict hydrolysis rates. *Bioresour. Technol.* **2010**, *101*, 4461–4471. [CrossRef]
123. Stanciu, M.-C.; Teacă, C.-A. Changes of Wood Surfaces Treated with Natural-based Products—Structural and Properties Investigation. *BioResources* **2024**, *19*, 5895–5915. [CrossRef]
124. Hinterstoisser, B.; Salmén, L. Application of dynamic 2D FTIR to cellulose. *Vib. Spectrosc.* **2000**, *22*, 111–118. [CrossRef]
125. Teacă, C.-A.; Bodîrlău, R.; Spiridon, I. Dissolution of natural polymers in ionic liquid. *Rev. Roum. Chim.* **2011**, *56*, 33–38.
126. Im, J.; Lee, S.; Jo, I.; Kang, J.W.; Kim, K.-S. Structural characteristics and thermal properties of regenerated cellulose, hemicellulose and lignin after being dissolved in ionic liquids. *J. Ind. Eng. Chem.* **2022**, *107*, 365–375. [CrossRef]
127. Krässig, H.A. *Cellulose: Structure, Accessibility, and Reactivity*; Huglin, M.B., Ed.; Gordon and Breach Science Pub.: Yverdon, Switzerland, 1993.
128. Kumar, P.; Barrett, D.M.; Delwiche, M.J.; Stroeve, P. Methods for pretreatment of lignocellulosic biomass for efficient hydrolysis and biofuel production. *Ind. Eng. Chem. Res.* **2009**, *48*, 3713–3729. [CrossRef]
129. Rinaldi, R.; Schüth, F. Acid hydrolysis of cellulose as the entry point into biorefinery schemes. *ChemSusChem* **2009**, *2*, 1096–1107. [CrossRef]
130. Alvira, P.; Tomás-Pejó, E.; Ballesteros, M.; Negro, M.J. Pretreatment technologies for an efficient bioethanol production process based on enzymatic hydrolysis: A review. *Bioresour. Technol.* **2010**, *101*, 4851–4861. [CrossRef]
131. Geboers, J.A.; Van de Vyver, S.; Ooms, R.; de Beeck, B.O.; Jacobs, P.A.; Sels, B.F. Chemocatalytic conversion of cellulose: Opportunities, advances and pitfalls. *Catal. Sci. Technol.* **2011**, *1*, 714–726. [CrossRef]
132. van de Vyver, S.; Geboers, J.; Jacobs, P.A.; Sels, B.F. Recent advances in the catalytic conversion of cellulose. *Chem. Cat. Chem.* **2011**, *3*, 82–94. [CrossRef]
133. Isogai, A.; Usuda, M. Crystallinity indexes of cellulosic materials. *Sen'i Gakkaishi* **1990**, *46*, 324–329. [CrossRef]
134. Lee, C.; Dazen, K.; Kafle, K.; Moore, A.; Johnson, D.K.; Park, S.; Kim, S.H. Correlations of apparent cellulose crystallinity determined by XRD, NMR, IR, Raman, and SFG methods. In *Cellulose Chemistry and Properties: Fibers, Nanocelluloses and Advanced Materials*; Rojas, O.J., Ed.; Springer: Cham, Switzerland, 2015. [CrossRef]
135. French, A.D. Idealized powder diffraction patterns for cellulose polymorphs. *Cellulose* **2014**, *21*, 885–896. [CrossRef]
136. Nishikawa, S.; Ono, S. Transmission of X-rays through fibrous, lamellar and granular substances. *Proc. Tokyo Math.-Phys. Soc.* **1913**, *7*, 131–138. [CrossRef]
137. Hermans, P.H.; Weidinger, A. Quantitative X-Ray investigations on the crystallinity of cellulose fibers. A background analysis. *J. Appl. Phys.* **1948**, *19*, 491–506. [CrossRef]
138. Hermans, P.H.; Weidinger, A. Quantitative investigation of the X-Ray diffraction picture of some typical rayon specimens: Part I. *Text. Res. J.* **1961**, *31*, 558–571. [CrossRef]
139. Ruland, W. X-ray determination of crystallinity and diffuse disorder scattering. *Acta Crystallogr.* **1961**, *14*, 1180–1185. [CrossRef]
140. Vonk, C. Computerization of Ruland's X-ray method for determination of the crystallinity in polymers. *J. Appl. Crystallogr.* **1973**, *6*, 148–152. [CrossRef]
141. Kafle, K.; Lee, C.; Shin, H.; Zoppe, J.; Johnson, D.; Kim, S.; Park, S. Effects of delignification on crystalline cellulose in lignocellulose biomass characterized by vibrational sum frequency generation spectroscopy and X-ray diffraction. *Bioenergy Res.* **2015**, *8*, 1750–1758. [CrossRef]

142. Hult, E.-L.; Iversen, T.; Sugiyama, J. Characterization of the supermolecular structure of cellulose in wood pulp fibres. *Cellulose* **2003**, *10*, 103–110. [CrossRef]
143. He, J.; Cui, S.; Wang, S.-Y. Preparation and crystalline analysis of high-grade bamboo dissolving pulp for cellulose acetate. *J. Appl. Polym. Sci.* **2008**, *107*, 1029–1038. [CrossRef]
144. Garvey, C.J.; Parker, I.H.; Simon, G.P. On the interpretation of X-Ray diffraction powder patterns in terms of the nanostructure of cellulose I fibres. *Macromol. Chem. Phys.* **2005**, *206*, 1568–1575. [CrossRef]
145. Ahvenainen, P.; Kontro, I.; Svedström, K. Comparison of sample crystallinity determination methods by X-ray diffraction for challenging cellulose I materials. *Cellulose* **2016**, *23*, 1073–1086. [CrossRef]
146. Nelson, M.L.; Conrad, C.M. Effect of grinding on the crystallinity of cellulose fibers, as indicated by the acid-hydrolysis and other techniques. *Textile Res. J.* **1948**, *18*, 155–164. [CrossRef]
147. Mayer-Laigle, C.; Blanc, N.; Rajaonarivony, R.K.; Rouau, X. Comminution of dry lignocellulosic biomass, a review: Part I. from fundamental mechanisms to milling behaviour. *Bioengineering* **2018**, *5*, 41. [CrossRef]
148. Mayer-Laigle, C.; Rajaonarivony, R.K.; Blanc, N.; Rouau, X. Comminution of dry lignocellulosic biomass: Part II. Technologies, improvement of milling performances, and security issues. *Bioengineering* **2018**, *5*, 50. [CrossRef]
149. Vehniäinen, A.; Haikkala, P.; Suhonen, T. Future outlook in papermaking science and technology. In *Mechanical Pulping*; Lönnberg, B., Ed.; Paper Engineers' Association/Paperi Ja Puu Oy: Helsinki, Finland, 2009; pp. 516–534.
150. Boissou, F.; Sayoud, N.; De Oliveira Vigier, K.; Barakat, A.; Marinkovic, S.; Estrine, B.; Jérôme, F. Acid-assisted ball milling of cellulose as an efficient pretreatment process for the production of butyl glycosides. *ChemSusChem* **2015**, *8*, 3263–3269. [CrossRef]
151. Hick, S.M.; Griebel, C.; Restrepo, D.T.; Truitt, J.H.; Buker, E.J.; Bylda, C.; Blair, R.G. Mechanocatalysis for biomass-derived chemicals and fuels. *Green Chem.* **2010**, *12*, 468–474. [CrossRef]
152. Ouajai, S.; Shanks, R. Solvent and enzyme induced recrystallization of mechanically degraded hemp cellulose. *Cellulose* **2006**, *13*, 31–44. [CrossRef]
153. Ribeiro, L.S.; Órfão, J.J.; Pereira, M.F.R. Enhanced direct production of sorbitol by cellulose ball-milling. *Green Chem.* **2015**, *17*, 2973–2980. [CrossRef]
154. Xu, H.; Che, X.; Ding, Y.; Kong, Y.; Li, B.; Tian, W. Effect of crystallinity on pretreatment and enzymatic hydrolysis of lignocellulosic biomass based on multivariate analysis. *Bioresour. Technol.* **2019**, *279*, 271–280. [CrossRef]
155. Shrotri, A.; Kobayashi, H.; Fukuoka, A. Air oxidation of activated carbon to synthesize a biomimetic catalyst for hydrolysis of cellulose. *ChemSusChem* **2016**, *9*, 1299–1303. [CrossRef]
156. Kobayashi, H.; Kaiki, H.; Shrotri, A.; Techikawara, K.; Fukuoka, A. Hydrolysis of woody biomass by a biomass-derived reusable heterogeneous catalyst. *Chem. Sci.* **2016**, *7*, 692–696. [CrossRef]
157. Betiku, E.; Adetunji, O.; Ojumu, T.; Solomon, B.A. Comparative study of the hydrolysis of gamma irradiated lignocelluloses. *Braz. J. Chem. Eng.* **2009**, *26*, 251–255. [CrossRef]
158. Bak, J.S. Electron beam irradiation enhances the digestibility and fermentation yield of water-soaked lignocellulosic biomass. *Biotechnol. Rep.* **2014**, *4*, 30–33. [CrossRef]
159. Remón, J.; Li, T.; Chuck, C.J.; Matharu, A.S.; Clark, J.H. Toward renewable-based, food-applicable prebiotics from biomass: A one-step, additive-free, microwave-assisted hydrothermal process for the production of high purity xylo-oligosaccharides from beech wood hemicellulose. *ACS Sustain. Chem. Eng.* **2019**, *7*, 16160–16172. [CrossRef]
160. Li, H.; Qu, Y.; Yang, Y.; Chang, S.; Xu, J. Microwave irradiation—A green and efficient way to pretreat biomass. *Bioresour. Technol.* **2016**, *199*, 34–41. [CrossRef]
161. Bussemaker, M.J.; Zhang, D. Effect of ultrasound on lignocellulosic biomass as a pretreatment for biorefinery and biofuel applications. *Ind. Eng. Chem. Res.* **2013**, *52*, 3563–3580. [CrossRef]
162. He, Z.; Wang, Z.; Zhao, Z.; Yi, S.; Mu, J.; Wang, X. Influence of ultrasound pretreatment on wood physiochemical structure. *Ultrason.Sonochem.* **2017**, *34*, 136–141. [CrossRef]
163. Benoit, M.; Rodrigues, A.; Zhang, Q.; Fourré, E.; De Oliveira Vigier, K.; Tatibouët, J.-M.; Jérôme, F. Depolymerization of cellulose assisted by a nonthermal atmospheric plasma. *Angew. Chem. Int. Ed.* **2011**, *50*, 8964–8967. [CrossRef]
164. Vanneste, J.; Ennaert, T.; Vanhulsel, A.; Sels, B. Unconventional pretreatment of lignocellulose with low-temperature plasma. *ChemSusChem* **2017**, *10*, 14–31. [CrossRef]
165. Yang, B.; Tao, L.; Wyman, C.E. Strengths, challenges, and opportunities for hydrothermal pretreatment in lignocellulosic biorefineries. *Biofuels Bioprod. Biorefining* **2018**, *12*, 125–138. [CrossRef]
166. Sturgeon, M.R.; Kim, S.; Lawrence, K.; Paton, R.S.; Chmely, S.C.; Nimlos, M.; Foust, T.D.; Beckham, G.T. A mechanistic investigation of acid-catalyzed cleavage of aryl-ether linkages: Implications for lignin depolymerization in acidic environments. *ACS Sustain. Chem. Eng.* **2013**, *2*, 472–485. [CrossRef]
167. Li, J.; Henriksson, G.; Gellerstedt, G. Lignin depolymerization/repolymer-ization and its critical role for delignification of aspen wood by steam explosion. *Bioresour. Technol.* **2007**, *98*, 3061–3068. [CrossRef] [PubMed]

168. Donohoe, B.S.; Decker, S.R.; Tucker, M.P.; Himmel, M.E.; Vinzant, T.B. Visualizing lignin coalescence and migration through maize cell walls following thermochemical pretreatment. *Biotechnol. Bioeng.* **2008**, *101*, 913–925. [CrossRef] [PubMed]
169. Deguchi, S.; Tsujii, K.; Horikoshi, K. Crystalline-to-amorphous transformation of cellulose in hot and compressed water and its implications for hydrothermal conversion. *Green Chem.* **2008**, *10*, 191–196. [CrossRef]
170. Silveira, R.L.; Stoyanov, S.R.; Kovalenko, A.; Skaf, M.S. Cellulose aggregation under hydrothermal pretreatment conditions. *Biomacromolecules* **2016**, *17*, 2582–2590. [CrossRef]
171. Sun, Y.G.; Ma, Y.; Wang, Z.; Yao, J. Evaluating and optimizing pretreatment technique for catalytic hydrogenolysis conversion of corn stalk into polyol. *Bioresour. Technol.* **2014**, *158*, 307–312. [CrossRef]
172. Trajano, H.L.; Wyman, C.E. Fundamentals of biomass pretreatment at low pH. In *Aqueous Pretreatment of Plant Biomass for Biological and Chemical Conversion to Fuels and Chemicals*; Wyman, C.E., Ed.; John Wiley and Sons, Ltd.: West Sussex, UK, 2013. [CrossRef]
173. Ramirez, R.S.; Holtzapple, M.; Piamonte, N. Fundamentals of biomass pretreatment at high pH. In *Aqueous Pretreatment of Plant Biomass for Biological and Chemical Conversion to Fuels and Chemicals*; Wyman, C.E., Ed.; John Wiley and Sons, Ltd.: West Sussex, UK, 2013; pp. 145–167. [CrossRef]
174. Meng, X.; Wells, T.; Sun, Q.; Huang, F.; Ragauskas, A. Insights into the effect of dilute acid, hot water or alkaline pretreatment on the cellulose accessible surface area and the overall porosity of Populus. *Green Chem.* **2015**, *17*, 4239–4246. [CrossRef]
175. Zhang, J.; Zhang, B.; Zhang, J.; Lin, L.; Liu, S.; Ouyang, P. Effect of phosphoric acid pretreatment on enzymatic hydrolysis of microcrystalline cellulose. *Biotechnol. Adv.* **2010**, *28*, 613–619. [CrossRef]
176. Deng, W.; Tan, X.; Fang, W.; Zhang, Q.; Wang, Y. Conversion of cellulose into sorbitol over carbon nanotube-supported ruthenium catalyst. *Catal. Lett.* **2009**, *133*, 167. [CrossRef]
177. Kootstra, A.M.; Beeftink, H.; Scott, E.; Sanders, J. Optimization of the dilute maleic acid pretreatment of wheat straw. *Biotechnol. Biofuels* **2009**, *2*, 31. [CrossRef]
178. Kootstra, A.M.; Beeftink, H.; Scott, E.; Sanders, J. Comparison of dilute mineral and organic acid pretreatment for enzymatic hydrolysis of wheat straw. *Biochem. Eng. J.* **2009**, *46*, 126–131. [CrossRef]
179. Scordia, D.; Cosentino, S.L.; Lee, J.-W.; Jeffries, T.W. Dilute oxalic acid pretreatment for biorefining giant reed (*Arundo donax* L.). *Biomass Bioenergy* **2011**, *35*, 3018–3024. [CrossRef]
180. Lam, H.Q.; Bigot, Y.L.; Delmas, M.; Avignon, E.G. Formic acid pulping of rice straw. *Ind. Crops Prod.* **2001**, *14*, 65–71. [CrossRef]
181. Young, R.A.; Davis, J.L.; Wiesmann, E.-B. Organic acid pulping of wood—Part II. Acetic acid pulping of aspen. *Holzforschung-Int. J. Biol. Chem. Phys. Technol. Wood* **1986**, *40*, 99–108. [CrossRef]
182. Ogasawara, Y.; Itagaki, S.; Yamaguchi, K.; Mizuno, N. Saccharification of natural lignocellulose biomass and polysaccharides by highly negatively charged heteropolyacids in concentrated aqueous solution. *ChemSusChem* **2011**, *4*, 519–525. [CrossRef]
183. Zhao, X.; Cheng, K.; Liu, D. Organosolv pretreatment of lignocellulosic biomass for enzymatic hydrolysis. *Appl. Microbiol. Biotechnol.* **2009**, *82*, 815–827. [CrossRef]
184. Akien, G.R.; Qi, L.; Horvath, I.T. Molecular mapping of the acid catalysed dehydration of fructose. *Chem. Commun.* **2012**, *48*, 5850–5852. [CrossRef]
185. Geboers, J.A.; Van de Vyver, S.; Carpentier, K.; Jacobs, P.; Sels, B. Hydrolytic hydrogenation of cellulose with hydrotreated caesium salts of heteropoly acids and Ru/C. *Green Chem.* **2011**, *13*, 2167–2174. [CrossRef]
186. Al-Zuhair, S. The effect of crystallinity of cellulose on the rate of reducing sugars production by heterogeneous enzymatic hydrolysis. *Bioresour. Technol.* **2008**, *99*, 4078–4085. [CrossRef]
187. Awa, K.; Shinzawa, H.; Ozaki, Y. The effect of microcrystalline cellulose crystallinity on the hydrophilic property of tablets and the hydrolysis of acetylsalicylic acid as active pharmaceutical ingredient inside tablets. *AAPS PharmSciTech* **2015**, *16*, 865–870. [CrossRef]
188. Dusselier, M.; Van Wouwe, P.; Dewaele, A.; Makshina, E.; Sels, B.F. Lactic acid as a platform chemical in the biobased economy: The role of chemocatalysis. *Energy Environ. Sci.* **2013**, *6*, 1415–1442. [CrossRef]
189. Hindi, S.S.Z. The interconvertibility of cellulose's allomorphs. *Int. J. Innov. Res. Sci. Eng. Technol.* **2016**, *6*, 715–722.
190. Carrillo-Varela, I.; Pereira, M.; Teixeira Mendonça, R. Determination of polymorphic changes in cellulose from *Eucalyptus* spp. fibres after alkalization. *Cellulose* **2018**, *25*, 6831–6845. [CrossRef]
191. Nishiyama, Y.; Chanzy, H.; Wada, M.; Sugiyama, J.; Mazeau, K.; Forsyth, T.; Riekel, C.; Mueller, M.; Rasmussen, B.; Langan, P. *Synchrotron X-Ray and Neutron Fiber Diffraction Studies of Cellulose Polymorphs*; LA-UR-01-4154; Los Alamos National Lab.: Los Alamos, NM, USA, 2001.
192. Wada, M.; Chanzy, H.; Nishiyama, Y.; Langan, P. Cellulose IIII crystal structure and hydrogen bonding by synchrotron X-ray and neutron fiber diffraction. *Macromolecules* **2004**, *37*, 8548–8555. [CrossRef]
193. Nam, S.; French, A.D.; Condon, B.D.; Concha, M. Segal crystallinity index revisited by the simulation of X-ray diffraction patterns of cotton cellulose Iβ and cellulose II. *Carbohydr. Polym.* **2016**, *135*, 1–9. [CrossRef]
194. Miao, X.; Tian, F.; Lin, J.; Li, H.; Li, X.; Bian, F.; Zhang, X. Tuning the mechanical properties of cellulose nanofibrils reinforced polyvinyl alcohol composites via altering the cellulose polymorphs. *RSC Adv.* **2016**, *6*, 83356–83365. [CrossRef]

195. Sousa, L.D.C.; Humpula, J.; Balan, V.; Dale, B.E.; Chundawat, S.P. Impact of ammonia pretreatment conditions on the cellulose III allomorph ultrastructure and its enzymatic digestibility. *ACS Sustain. Chem. Eng.* **2019**, *7*, 14411–14424. [CrossRef]
196. Mittal, A.; Katahira, R.; Himmel, M.; Johnson, D. Effects of alkaline or liquid-ammonia treatment on crystalline cellulose: Changes in crystalline structure and effects on enzymatic digestibility. *Biotechnol. Biofuels* **2011**, *4*, 41. [CrossRef]
197. Balan, V.; Bals, B.; Chundawat, S.P.S.; Marshall, D.; Dale, B.E. Lignocellulosic biomass pretreatment using AFEX. In *Biofuels. Methods in Molecular Biology (Methods and Protocols)*; Mielenz, J., Ed.; Humana Press: Totowa, NJ, USA, 2009. [CrossRef]
198. Chundawat, S.P.S.; Donohoe, B.S.; da Costa Sousa, L.; Elder, T.; Agarwal, U.P.; Lu, F.; Ralph, J.; Himmel, M.E.; Balan, V.; Dale, B.E. Multi-scale visualization and characterization of lignocellulosic plant cell wall deconstruction during thermochemical pretreatment. *Energy Environ. Sci.* **2011**, *4*, 973–984. [CrossRef]
199. da Costa Sousa, L.; Jin, M.; Chundawat, S.P.; Bokade, V.; Tang, X.; Azarpira, A.; Lu, F.; Avci, U.; Humpula, J.; Uppugundla, N. Next-generation ammonia pretreatment enhances cellulosic biofuel production. *Energy Environ. Sci.* **2016**, *9*, 1215–1223. [CrossRef]
200. Avci, U.; Zhou, X.; Pattathil, S.; Leonardo, S.D.; Hahn, M.G.; Dale, B.; Xu, Y.; Balan, V. Effects of extractive ammonia pretreatment on the ultrastructure and glycan composition of corn stover. *Front. Energy Res.* **2019**, *7*, 85. [CrossRef]
201. Ferrini, P.; Rinaldi, R. Catalytic biorefining of plant biomass to non-pyrolytic lignin bio-oil and carbohydrates through hydrogen transfer reactions. *Angew. Chemie Int. Ed.* **2014**, *53*, 8634–8639. [CrossRef]
202. Galkin, M.V.; Samec, J.S. Selective route to 2-propenyl aryls directly from wood by a tandem organosolv and palladium-catalysed transfer hydrogenolysis. *ChemSusChem* **2014**, *7*, 2154–2158. [CrossRef] [PubMed]
203. van den Bosch, S.; Schutyser, W.; Vanholme, R.; Driessen, T.; Koelewijn, S.-F.; Renders, T.; De Meester, B.; Huijgen, W.; Dehaen, W.; Courtin, C. Reductive lignocellulose fractionation into soluble lignin-derived phenolic monomers and dimers and processable carbohydrate pulps. *Energy Environ. Sci.* **2015**, *8*, 1748–1763. [CrossRef]
204. Renders, T.; Van den Bosch, S.; Vangeel, T.; Ennaert, T.; Koelewijn, S.-F.; Van den Bossche, G.; Courtin, C.M.; Schutyser, W.; Sels, B.F. Synergetic effects of alcohol/water mixing on the catalytic reductive fractionation of poplar wood. *ACS Sustain. Chem. Eng.* **2016**, *4*, 6894–6904. [CrossRef]
205. Renders, T.; Cooreman, E.; Van den Bosch, S.; Schutyser, W.; Koelewijn, S.-F.; Vangeel, T.; Deneyer, A.; Van den Bossche, G.; Courtin, C.; Sels, B. Catalytic lignocellulose biorefining in n-butanol/water: A one-pot approach toward phenolics, polyols, and cellulose. *Green Chem.* **2018**, *20*, 4607–4619. [CrossRef]
206. Sun, J.; Li, H.; Xiao, L.-P.; Guo, X.; Fang, Y.; Sun, R.-C.; Song, G. Fragmentation of woody lignocellulose into primary monolignols and their derivatives. *ACS Sustain.Chem. Eng.* **2019**, *7*, 4666–4674. [CrossRef]
207. Renders, T.; Schutyser, W.; Van den Bosch, S.; Koelewijn, S.-F.; Vangeel, T.; Courtin, C.M.; Sels, B.F. Influence of acidic (H3PO4) and alkaline (NaOH) additives on the catalytic reductive fractionation of lignocellulose. *ACS Catal.* **2016**, *6*, 2055–2066. [CrossRef]
208. Singh, S.; Simmons, B.A. Ionic liquid pretreatment: Mechanism, performance, and challenges. In *Aqueous Pretreatment of Plant Biomass for Biological and Chemical Conversion to Fuels and Chemicals*; Wyman, C.E., Ed.; John Wiley and Sons, Ltd.: West Sussex, UK, 2013. [CrossRef]
209. Cao, Y.; Li, H.; Zhang, Y.; Zhang, J.; He, J. Structure and properties of novel regenerated cellulose films prepared from cornhusk cellulose in room temperature ionic liquids. *J. Appl. Polym. Sci.* **2010**, *116*, 547–554. [CrossRef]
210. Zhao, Q.; Yam, R.C.; Zhang, B.; Yang, Y.; Cheng, X.; Li, R.K. Novel all-cellulose ecocomposites prepared in ionic liquids. *Cellulose* **2009**, *16*, 217–226. [CrossRef]
211. Lee, S.H.; Doherty, T.V.; Linhardt, R.J.; Dordick, J.S. Ionic liquid-mediated selective extraction of lignin from wood leading to enhanced enzymatic cellulose hydrolysis. *Biotechnol. Bioeng.* **2009**, *102*, 1368–1376. [CrossRef]
212. Kim, S.-J.; Dwiatmoko, A.A.; Choi, J.W.; Suh, Y.-W.; Suh, D.J.; Oh, M. Cellulose pretreatment with 1-n-butyl-3-methylimidazolium chloride for solid acid-catalyzed hydrolysis. *Bioresour. Technol.* **2010**, *101*, 8273–8279. [CrossRef]
213. Dibble, D.C.; Li, C.; Sun, L.; George, A.; Cheng, A.; Cetinkol, O.P.; Benke, P.; Holmes, B.M.; Singh, S.; Simmons, B.A. A facile method for the recovery of ionic liquid and lignin from biomass pretreatment. *Green Chem.* **2011**, *13*, 3255–3264. [CrossRef]
214. Zavrel, M.; Bross, D.; Funke, M.; Büchs, J.; Spiess, A.C. High-throughput screening for ionic liquids dissolving (ligno-)cellulose. *Bioresour. Technol.* **2009**, *100*, 2580–2587. [CrossRef]
215. Sun, S.; Sun, S.; Cao, X.; Sun, R. The role of pretreatment in improving the enzymatic hydrolysis of lignocellulosic materials. *Bioresour. Technol.* **2016**, *199*, 49–58. [CrossRef]
216. Sakamoto, Y.; Imamura, K.; Onda, A. Hydrolysis of oligosaccharides and polysaccharides on sulfonated solid acid catalysts: Relations between adsorption properties and catalytic activities. *ACS Omega* **2020**, *5*, 24964–24972. [CrossRef]
217. Zeng, M.; Pan, X. Insights into solid acid catalysts for efficient cellulose hydrolysis to glucose: Progress, challenges, and future opportunities. *Catal. Rev. Sci. Eng.* **2022**, *64*, 445–490. [CrossRef]
218. Rinaldi, R.; Meine, N.; vom Stein, J.; Palkovits, R.; Schüth, F. Which controls the depolymerization of cellulose in ionic liquids: The solid acid catalyst or cellulose? *ChemSusChem* **2010**, *3*, 266–276. [CrossRef]

219. Rinaldi, R.; Palkovits, R.; Schüth, F. Depolymerization of cellulose using solid catalysts in ionic liquids. *Angew. Chemie Int. Ed.* **2008**, *47*, 8047–8050. [CrossRef]
220. Zakzeski, J.; Grisel, R.J.; Smit, A.T.; Weckhuysen, B.M. Solid acid-catalyzed cellulose hydrolysis monitored by in situ ATR-IR spectroscopy. *ChemSusChem* **2012**, *5*, 430–437. [CrossRef]
221. Grisel, R.J.H.; Smit, A.T. Thermochemical saccharification of cellulose: The benefit of adding a scavenger. *Appl. Catal. A Gen.* **2014**, *475*, 438–445. [CrossRef]
222. Groff, D.; George, A.; Sun, N.; Sathitsuksanoh, N.; Bokinsky, G.; Simmons, B.A.; Holmes, B.M.; Keasling, J.D. Acid enhanced ionic liquid pretreatment of biomass. *Green Chem.* **2013**, *15*, 1264–1267. [CrossRef]
223. Zheng, W.; Cui, Y.; Xu, Z.; Zhao, L.; Sun, W. Cellulose transformation into methyl glucosides catalyzed by H3PW12O40: Enhancement of ionic liquid pretreatment. *Can. J. Chem. Eng.* **2018**, *96*, 1250–1255. [CrossRef]
224. Sun, J.; Konda, N.M.; Parthasarathi, R.; Dutta, T.; Valiev, M.; Xu, F.; Simmons, B.A.; Singh, S. One-pot integrated biofuel production using low-cost biocompatible protic ionic liquids. *Green Chem.* **2017**, *19*, 3152–3163. [CrossRef]
225. Xu, F.; Sun, J.; Konda, N.M.; Shi, J.; Dutta, T.; Scown, C.D.; Simmons, B.A.; Singh, S. Transforming biomass conversion with ionic liquids: Process intensification and the development of a high-gravity, one-pot process for the production of cellulosic ethanol. *Energy Environ. Sci.* **2016**, *9*, 1042–1049. [CrossRef]
226. Shi, J.; Gladden, J.M.; Sathitsuksanoh, N.; Kambam, P.; Sandoval, L.; Mitra, D.; Zhang, S.; George, A.; Singer, S.W.; Simmons, B.A.; et al. One-pot ionic liquid pretreatment and saccharification of switchgrass. *Green Chem.* **2013**, *15*, 2579–2589. [CrossRef]
227. Shi, J.; Balamurugan, K.; Parthasarathi, R.; Sathitsuksanoh, N.; Zhang, S.; Stavila, V.; Subramanian, V.; Simmons, B.A.; Singh, S. Understanding the role of water during ionic liquid pretreatment of lignocellulose: Co-solvent or anti-solvent? *Green Chem.* **2014**, *16*, 3830–3840. [CrossRef]
228. Kim, K.H.; Eudes, A.; Jeong, K.; Yoo, C.G.; Kim, C.S.; Ragauskas, A. Integration of renewable deep eutectic solvents with engineered biomass to achieve a closed loop biorefinery. *Proc. Natl. Acad. Sci. USA* **2019**, *116*, 13816–13824. [CrossRef]
229. Socha, A.M.; Parthasarathi, R.; Shi, J.; Pattathil, S.; Whyte, D.; Bergeron, M.; George, A.; Tran, K.; Stavila, V.; Venkatachalam, S. Efficient biomass pretreatment using ionic liquids derived from lignin and hemicellulose. *Proc. Natl. Acad. Sci. USA* **2014**, *111*, E3587–E3595. [CrossRef]
230. Široký, J.; Blackburn, R.S.; Bechtold, T.; Taylor, J.; White, P. Attenuated total reflectance Fourier-transform Infrared spectroscopy analysis of crystallinity changes in lyocell following continuous treatment with sodium hydroxide. *Cellulose* **2010**, *17*, 103–115. [CrossRef]

Disclaimer/Publisher's Note: The statements, opinions and data contained in all publications are solely those of the individual author(s) and contributor(s) and not of MDPI and/or the editor(s). MDPI and/or the editor(s) disclaim responsibility for any injury to people or property resulting from any ideas, methods, instructions or products referred to in the content.